DIRECTION DU CYCLE DU COMBUSTIBLE

DEPARTEMENT DU RETRAITEMENT, DES DECHETS ET DU DEMANTELEMENT

NOTE TECHNIQUE : NT/SCD/N° 95.03

TITRE : **Effect of geologic repository parameters on aqueous corrosion of nuclear glass.**
Corrosion aqueuse des verres nucléaires en fonction des paramètres de stockage géologique.
(Contrat CCE FI 2W CT90 0027. Rapport annuel 1994).

Auteurs : I.TOVENA, T.ADVOCAT, P.JOLLIVET, N.GODON, E.VERNAZ.

COMMISSION DES
COMMUNAUTES EUROPEENNES

At the present stage of this investigation, it is impossible to predict the effects of the glass composition on the long-term behavior. Corrosion experiments with glass powder samples thus continue to remain the only quantitative means of estimating long-term glass stability.

6. CONCLUSIONS

Twenty aluminoborosilicate glass compositions containing simulated fission product oxides were defined using the experimentation plan methodology. Three additional glass compositions were also tested.

Monolithic glass corrosion tests in a dilute aqueous medium at 90°C indicated the variation range for the initial corrosion rates r_0. Significant but only qualitative correlations were established between the initial corrosion rate and the molar fraction of glass network forming oxides ($SiO_2 + Al_2O_3$), and between the initial rate and the $(Na_2O + Li_2O + B_2O_3) / (SiO_2 + Al_2O_3)$ molar ratio in the glass. The experimentation plan allowed a polynomial model to be defined relating the initial corrosion rate at 90°C to the oxide concentrations in the glass. Although the model is theoretically capable of predicting the corrosion rates, it does not always account for the actual data measured during other experiments; this discrepancy may be attributable either to the presence of other chemical elements (MgO) or to CaO concentrations differing from the fixed value adopted for the experimentation plan. Considering the current (partial) results obtained, the pertinence of the experimentation plan for a very wide range of glass compositions may be called into question; would it not be preferable to adopt this strategy for composition subsets specified for more limited composition ranges?

Glass powder corrosion tests designed to simulate advanced corrosion reaction progress, account for the wide variations in the dissolved glass quantities, although no correlation exists with the glass chemical composition. At the current stage of the investigation it is too early to conclude. Still unanswered questions include the role of secondary alteration products in controlling the composition of the alteration solution, and the kinetic law governing all the glass compositions tested. The partial results available at this time cast doubts on the pertinence of a rate law in which the reaction affinity is based exclusively on the orthosilicic acid activity in solution.

49 refs. 4 Figs. 36 Tabs.

CEA
DIRECTION DU CYCLE DU COMBUSTIBLE
DEPARTEMENT DU RETRAITEMENT, DES DECHETS ET DU DEMANTELEMENT
SERVICE DE CONFINEMENT DES DECHETS
Section de Développement des Matériaux de Confinement

Programme CEA	N° 95	Libellé
FA rang 3	682	Caractérisation et comportement à long terme
FA rang 4	6821	verres
Segment	17	stockage et entreposage
Sous-Segment		comportement à long terme
Collaborations	**95**	
COGEMA		
ANDRA		
EDF		
CCE	**Contrat FI 2W CT90 0027**	

NOTE TECHNIQUE : NT/SCD/N° 95.03

TITRE : Effect of geologic repository parameters on aqueous corrosion of nuclear glass.

Corrosion aqueuse des verres nucléaires en fonction des paramètres de stockage géologique.
(Contrat CCE FI 2W CT90 0027. Rapport annuel 1994).

Auteurs : I.TOVENA, T.ADVOCAT, P.JOLLIVET, N.GODON, E.VERNAZ.

Qualité	*Noms*	*Visas*	*Date*
Auteurs	I. TOVENA T.ADVOCAT		13/2/95 13/2/95
Vérificateurs	N. JACQUET-FRANCILLON E. VERNAZ		24/2/95 20/2/95
Chef de Service	J.P. MONCOUYOUX		27.2.95

CENTRE D'ETUDES DE LA VALLEE DU RHONE
BP 171 - 30207 BAGNOLS SUR CEZE CEDEX

CEA
DIRECTION DU CYCLE DU COMBUSTIBLE
DEPARTEMENT DU RETRAITEMENT, DES DECHETS ET DU DEMANTELEMENT
SERVICE DE CONFINEMENT DES DECHETS
Section de Développement des Matériaux de Confinement

Mots Clés : verres aluminoborosilicatés - corrosion - durabilité - plan d'experiences.

NOTE TECHNIQUE : NT/SCD/95.03

TITRE : **Effect of geologic repository parameters on aqueous corrosion of nuclear glass.**
Corrosion aqueuse des verres nucléaires en fonction des paramètres de stockage géologique.
(Contrat CCE FI 2W CT90 0027. Rapport annuel 1994).

AUTEURS : I. TOVENA, T. ADVOCAT, P. JOLLIVET, N. GODON, E. VERNAZ

RESUME :

Cette note constitue le rapport annuel 1994 du contrat CCE FI 2W CT 90 0027. Elle expose notamment les résultats obtenus sur la corrosion aqueuse à 90°C de 23 verres inactifs alumino-borosilicatés de sodium, adaptés au confinement de solutions de produits de fission type « Eau-Légère ». Des relations entre composition et durabilité dans l'eau des 23 verres ont été établies, principalement à partir des mesures de vitesses de corrosion initiales. Cette étude permet ainsi de fixer les tendances d'évolution de la durabilité des matrices vitreuses en fonction de leurs compositions.

CEA
DIRECTION DU CYCLE DU COMBUSTIBLE
DEPARTEMENT DU RETRAITEMENT, DES DECHETS ET DU DEMANTELEMENT
SERVICE DE CONFINEMENT DES DECHETS
Section de Développement des Matériaux de Confinement

ARCHIVAGE CIDRA

Classe du Document [0]

Type de document [NT]

Nombre de :

- Pages	41
- Tableaux	34
- Figures	4
- Planches	0
- Annexe	0
- Réf. Biblio	49

Descripteurs : verres alumino-borosilicatés - corrosion - durabilité - plan d'experiences

NOTE TECHNIQUE : NT/SCD/95.03

TITRE : **Effect of geologic repository parameters on aqueous corrosion of nuclear glass.**
Corrosion aqueuse des verres nucléaires en fonction des paramètres de stockage géologique.
(Contrat CCE FI 2W CT90 0027. Rapport annuel 1994).

AUTEURS : I. TOVENA, T. ADVOCAT, P. JOLLIVET, N. GODON, E. VERNAZ

DESCRIPTIF :
Cette note présente le rapport annuel du contrat CCE FI 2W CT900027. Un état d'avancement du programme d'étude est présenté. Dans une seconde partie, les travaux relatifs aux relations entre la composition des verres et leur durabilité chimique sont exposés en détail.

Programme CEA	N° 95	Libellé
FA rang 3	682	Caractérisation et comportement à long terme
FA rang 4	6821	Verres
Segment	17	Stockage et entreposage
Sous-Segment		Comportement à long terme
Collaborations	95	
COGEMA		
ANDRA		
EDF		
CCE	**Contrat FI2W CT90 0027**	

SOMMAIRE

1. PROGRESS OF WORK AND OBTAINED RESULTS

1.1 Task B1: Basic Research on Aqueous Corrosion of Nuclear Glass

1.1.1 Effect of Glass Composition

The effects of MgO and SiO_2 on the aqueous corrosion stability of the glass were discussed in the 1991 Annual Report.

The effects of the Na_2O, B_2O_3, Al_2O_3 and fission product oxide concentrations on glass corrosion were investigated through experiments with glass monoliths at low glass surface-area-to-solution-volume (SA/V) ratios (10 m^{-1}) and with glass powder at high SA/V ratios (20 000 m^{-1}). Twenty glass compositions were selected by statistical methods, within the following composition ranges:

- SiO_2 concentration: 30–70 wt%
- Al_2O_3 concentration: 2–20 wt%
- B_2O_3 concentration: 7–20 wt%
- $Na_2O + Li_2O$ concentration: 9–24 wt%
- $Fe_2O_3 + NiO + Cr_2O_3 + P_2O_5$ concentration: 2.5–10 wt%
- Fission product oxides + actinide oxides + ZrO_2 concentration: 5–25 wt%

This part of the work program is discussed in the 1994 Annual Report (§.2 to §.6).

1.1.2 Role of External Ions

- *Effect of Anions and Cations*

The effects of metallic cations (Al, Fe, Zn, Pb and Mg) on the corrosion kinetics of R7T7 glass were the subjects of the 1994 Semiannual Report.

Tests were conducted at low SA/V ratios under static conditions at imposed pH values (acidic media at pH 2.9 and basic media at pH 8.9), using a single cell from which all solution samples were taken. The initial solution was double-distilled water to which metallic cations were added in variable concentrations. The highly diluted test medium corresponded to a very slight degree of reaction progress, allowing us to investigate the effects of the cations on the initial glass dissolution rate r_0.

At concentrations of 2.5×10^{-3} M, B, Na, Ca, K, Cl^-, NO_3^-, CO_3^{2-}, SO_4^{2-} did not induce major variations in the initial dissolution rate in basic media. In acid media at concentrations of 2.5×10^{-3} M, SO_4^{2-} and NO_3^- ions caused the initial rate to increase slightly (by factors of 3 and 1.4, respectively) while with $H_2PO_4^-$ ions the rate diminished by a factor of 4; F ions increased the initial rate by a factor of 4 at concentrations of 2.5×10^{-4} M, and by a factor of 30 at 2.5×10^{-3} M.

Tests were also conducted at high SA/V ratios using glass powder with flowing solution. The inflowing solution contained H_4SiO_4 at 90% of the saturation value with respect to the glass, as well as variable concentrations of metallic cations (Al, Fe, Zn). The high degree of reaction progress allowed us to assess the effect of cations on the glass dissolution rate under near-saturation conditions. the results clearly showed the kinetically limiting properties of aluminum.

- *Effect of Canister Corrosion Products*

A number of the R7T7 glass dissolution experiments in the presence of corrosion products from the NS24 (PC) steel canister have been completed and the alteration solutions analyzed. The results were discussed in the 1992 Semiannual Report.

The experiments on the effects of simple oxides and hydroxides (Fe, Ni, Cr and Ti) have been completed, as have the tests to assess the effects of the temperature (50°C and 70°C) and the

presence of "siliceous" additives (smectite, bentonite and silica gel). The test results are now being interpreted, and will be published in a later report.

- *Effect of Ionic Strength*

The effect of the ionic strength on the initial corrosion rate is now being investigated. R7T7 glass corrosion experiments were conducted with the following brine solutions: NaCl, Na_2SO_4, $MgCl_2$, $MgSO_4$, $CaCl_2$ and $CaSO_4$. The results will be discussed in the next report.

Investigation of the Interface Gel

The R7T7 glass alteration gels are currently being analyzed.

1.2 Task B2: Influence of the Disposal Site

1.2.1 Equilibrium Limits with Various Host Materials

Experiments to determine the equilibrium limits of R7T7 glass in the presence of 5 environmental materials (granite, two clays, schist and salt) were conducted at 90°C with an SA/V ratio of 5800 m^{-1} for durations of 7 days to 1 year. All the experiments have been completed and the results have been analyzed (they will be presented in a later report).

The first results show that each medium imposes a different pH, different elemental concentrations in solution, and different degrees of glass corrosion. Although the two clay media were the most aggressive with respect to R7T7 glass during the first six months, very low corrosion rates were reached after one year in all the test media.

At the present time, no direct relation has been established between the pH, the Si concentrations and the glass corrosion rates.

1.2.2 Parameter Experiments at 90°C

- *Alteration in the Presence of Schist*

The results of this investigation were discussed in the 1992 Annual Report.

- *Alteration in the Presence of Clay*

R7T7 glass alteration in two natural clays sampled from deep underground sites was studied for 1, 2, 3 and 6 months at 90°C. The clay was ultracentrifuged after the test to recover the leachate and perform elemental determinations and pH measurements. The results of this investigation will be presented in a later report.

- *Alteration in the Presence of Granite*

The results of this investigation were discussed in the 1992 Annual Report.

- *Alteration in the Presence of Salt*

R7T7 glass corrosion tests are currently in progress with two types of salt, at temperatures of 90°C and 150°C, at an SA/V ratio of 70 m^{-1} for durations of 7, 14, 28, 42, 56, 70, 84, 91, 120 and 180 days and for 1 and 2 years. Only the 1 and 2-year tests have not yet been completed. The alteration solutions have been analyzed and the crystallized phases identified by X-ray diffraction.

1.2.3 Integral Experiments

The "TAV 6" experiment simulating a granite repository environment has been in progress for over 11 years. Glass alteration remains very slight, and is controlled by the pseudo-flow due to the solution sampling procedure.

Four integral clay tests were initiated in 1992: two of them were terminated after 6 months, and the others after 2 years. Two integral schist tests were also initiated in 1992 for periods of 6 months and 2 years.

disposal concept selected for these tests was discussed in the 1992 Annual Report. Two of these tests were terminated after 8 months, and the other two after 24 months.
Schist: a TAV experiment was initiated in November 1992, and a second began in January 1994. The results of the TAV tests will be presented at a later date, when all the experimental findings are available.

1.3 Task B3: Development of a Glass Behavior Model

1.3.1 Mechanistic Model

This model was discussed in the 1993 Semiannual Report. The effects of the major parameters were quantified by simulations at 90°C using the LIXIVER code. The pH affects the glass solubility C^* and thus has only a very limited influence at values below 9. The apparent silicon diffusion coefficient in the alteration film proved to be the most sensitive parameter taken into account by the LIXIVER code: very slight D variations result in very different calculated element concentrations. A comparison between the calculated and experimental results showed that it was impossible to fit the short-term (up to 90-day) values using only a single diffusion coefficient for the entire experimental period.

1.3.2 Geochemical Model

The results of geochemical modeling with the KINDIS code (thermodynamic and kinetic constraints) of R7T7 glass at 90°C in water in contact with clay, and in contact with flowing water, were presented in detail in the 1993 Annual Report.

2. INTRODUCTION:
INVESTIGATING THE EFFECTS OF THE GLASS COMPOSITION

The French R7T7 borosilicate glass developed as a containment matrix for fission product solutions generated by reprocessing LWR fuel contains about thirty oxides; the major oxides or oxide groups are the following:

- SiO_2, B_2O_3, Al_2O_3, Na_2O+Li_2O, CaO
- Additive oxides (Fe_2O_3, NiO, Cr_2O_3, P_2O_5)
- ZrO_2
- Fission product and actinide oxides.

Sensitivity tests have been conducted in the past[1,2,3,4,5,6,7,8,9] to specify glass composition variations acceptable from the standpoints of technological feasibility, homogeneity and especially chemical durability. The acceptable composition range ("A") for R7T7 glass is the following:

- SiO_2 concentration: 42.4–51.7 wt%
- Al_2O_3 concentration: 3.6–6.6 wt%
- B_2O_3 concentration: 12.4–16.5 wt%
- $Na_2O + Li_2O$ concentration: 9.7–13.4 wt%
- Additive oxide ($Fe_2O_3 + NiO + Cr_2O_3$) concentration: 0–4.5 wt%
- Fission product + actinide oxide + ZrO_2 concentration: 4.2–18.5 wt%
- CaO concentration: 3.5–4.8 wt%

A wider range ("B") was considered for the purposes of this study:

- SiO_2 concentration: 30–70 wt%
- Al_2O_3 concentration: 2–20 wt%
- B_2O_3 concentration: 7–20 wt%
- $Na_2O + Li_2O$ concentration: 9–24 wt%
- Additive oxide concentration: 2.5–10 wt%
- Fission product oxide + actinide oxide + ZrO_2 concentration: 5–25 wt%

The fission product oxide spectrum was the same as for R7T7 glass, and the CaO concentration was 4 wt%.

Twenty glass compositions were specified within range "B" using the experimentation plan methodology (refer to § 4.5 on page 14). Three additional glass compositions previously specified by Tovena *et al.*[10] and included in range "A" were also tested. The initial corrosion rates r_0 were measured for the 23 glass compositions at 90°C in a dilute aqueous medium; the long-term corrosion rates were also measured on powder samples at 90°C in initially pure water with an SA/V ratio of 200 cm^{-1}.

The purpose of these two tests was to assess the effects of the glass composition on the initial corrosion rate and on the rate under near-saturation conditions. It is indispensable to determine the evolution of the corrosion kinetics with the reaction progress, and the solubility limits and corresponding low corrosion rates. Another objective of this investigation was to identify the glass corrosion mechanisms.

3. SELECTION OF THE 23 GLASS COMPOSITIONS

3.1 R7T7, R7T7$_{max}$ and R7T7$_{min}$

The R7T7 reference glass and two variants, designated R7T7$_{min}$ and R7T7$_{max}$, were tested. The variants correspond to the compositions with the minimum and maximum initial corrosion rates within range "A", based on the following empirical relation[10]:

$$\log r_0 = 0.022\ \Delta H + 8.246 \qquad (1)$$

where ΔH is the glass formation enthalpy (kcal·mol^{-1}) calculated from the hypotheses advanced by Feng and Barkatt[11] and r_0 is the initial dissolution rate measured over 28 days under Soxhlet conditions at 100°C.

The R7T7, R7T7$_{min}$ and R7T7$_{max}$ glass compositions are indicated in Table I.

3.2 Twenty Glass Compositions: IT1 to IT20

3.2.1 Composition Variation Ranges for Glass Component Oxides

Aluminoborosilicate glass for fission product containment contains about thirty oxides, comprising six main groups:

- SiO_2
- Al_2O_3
- $Na_2O + Li_2O$
- B_2O_3
- Additive oxides (Fe_2O_3, NiO, Cr_2O_3, P_2O_5)
- Fission product oxides and actinide oxides, together with ZrO_2

The problem was simplified by adopting a fixed percentage (4 wt%) for CaO.

3.2.1.1 SiO_2: 30–70 wt%

Silica is the primary network forming oxide in current nuclear containment glasses. A wide range of SiO_2 percentage variations was investigated to assess the long-term behavior of as many of the compositions as possible. Nuclear containment glasses with low SiO_2 concentrations include the "SAN" glass formulations. The industrial development of future high-temperature glass compositions[12] incorporating high SiO_2 concentrations depends on the implementation of the direct induction cold crucible melting process; these glasses have very high viscosities, but may exhibit very high chemical resistance.

3.2.1.2 Al_2O_3: 2–20 wt%

Alumina significantly effects the long-term glass dissolution kinetics[13]. Moreover, the high (16 wt%) Al_2O_3 concentration in natural basalt "SAN" glasses accounts for their refractory properties and high chemical resistance, and we therefore decided to investigate Al_2O_3 concentrations of up to 20 wt%. To assess the effect of alumina on limiting phase separation between the borate and silicate network[14,15,16], glass compositions with low Al_2O_3 concentrations were also studied.

3.2.1.3 $Na_2O + Li_2O$: 9–24 wt%

The alkali metals are known to diminish the viscosity, mechanical strength and chemical resistance of glass. In investigating compositions with large percentages of alkali metals, our objective was to determine their behavior during dissolution when the dissolved silica concentration reaches saturation and inhibits further corrosion of the silicate network.

3.2.1.4 B_2O_3: 2–20 wt%

Variations in the B_2O_3 content were examined to assess the effect of 3- or 4-coordinate boron on glass leaching resistance[17,18], and the effect of possible segregation within the borosilicate glass on its chemical resistance[19,20,21].

3.2.1.5 Additive Oxides: 2.5–10 wt%

Additive oxides are byproducts of the industrial fission product vitrification process, and include P_2O_5 (a solvent degradation product) as well as Fe_2O_3, NiO, Cr_2O_3 and ZnO (corrosion products). These oxides are crystal nucleation agents, and were investigated as such to evaluate the effects of crystallinity on the chemical durability of nuclear glass.

3.2.1.6 Fission Product Oxides + ZrO_2: 5–25 wt%

The goal of nuclear containment glass producers is to minimize the volume of the glass packages for disposal. One way to achieve this goal is to incorporate a higher percentage of fission product oxides in the vitrification process. This investigation therefore covered glass compositions with high percentages of simulated fission product oxides corresponding to the R7T7 spectrum[4,22] with the primary objective of identifying the impact of these oxides on the chemical durability of the matrix, and of measuring the radionuclide retention capacity of the alteration film.

3.2.2 Experimentation Plan Methodology

3.2.2.1 Rationale

It is difficult to identify the effect of a single oxide on a property such as the chemical durability of a nuclear glass with over thirty components. Conventional methods of addressing these mixture problems consist in replacing a given quantity of one oxide by other oxides[23,24,25,26], or in varying the percentage of one oxide and modifying the percentages of all the other oxides proportionally to their concentrations in the reference glass[27,28].

Our approach involved the experimentation plan methodology, which has a number of major advantages over such methods, notably greater efficiency in limiting the number of glass compositions necessary, and greater reliability by the optimized distribution of the mixtures over the specified composition range. This procedure provides for a higher degree of confidence in estimates of the effects of different oxides or models of glass properties, since the proportions of all the oxides vary from one composition to the next.

The main drawback of the method is its necessarily overall approach: i.e., all the compositions specified by the experimentation plan must be fabricated for purposes of modeling or identifying the effects of certain oxides. Moreover, the glass properties do not always vary continuous with variations in composition; this may limit the pertinence of the experimentation plan.

3.2.2.2 The Mixture Plan

Mixture problems are characterized by an additive mixing law:

$$\sum_{i \le k} X_i = 1$$

where X_i is the weight or molar fraction of oxide i, and k the number of factors (oxides). A polynomial model of degree 1 or 2 is most often used for mixture problems.

Defining an experimental matrix in a given experimentation range is a complex procedure. The necessary matrix optimality criteria are known, and require that the experimental points defined by the experimentation plan correspond to a particular symmetric distribution with a certain regularity

in the factor space. The extreme vertices plan devised by McLean and Anderson[29] appears to be the best suited for factor mixtures.

❖ *Experimental Matrix*

The problem may be summarized as follows:

- Factors: 6 oxide groups (SiO_2, Al_2O_3, B_2O_3, Na_2O+Li_2O, additive oxides, fission product and actinide oxides + ZrO_2).
- Experimental range: an irregular 5-dimensional hyperpolyhedron with 46 vertices, 119 edges and 1 center of gravity; the number of test points is therefore 47.
- The postulated model is an incomplete second-degree model, in that it only includes the quadratic terms for SiO_2. Prior studies on American nuclear glass compositions[30,31,32,33,34,35] have shown that a linear model is inadequate, but a second-degree polynomial model would have required a larger number of glass samples (36 compositions to investigate 6 oxides).

$$Y = b_1 \times (SiO_2) + b_2 \times (Al_2O_3) + b_3 \times (B_2O_3) + b_4 \times (Na_2O + Li_2O) + b_5 \times (\text{additive oxides}) + b_6 \times (\text{FP \& actinide oxides} + ZrO_2) + b_{12} \times (SiO_2 \times Al_2O_3) + b_{13} \times (SiO_2 \times B_2O_3) + b_{14} \times (SiO_2 \times (Na_2O + Li_2O)) + b_{15} \times (SiO_2 \times \text{additive oxides}) + b_{16} \times (SiO_2 \times (\text{FP \& actinide oxides} + ZrO_2))$$

The maximum number of glass compositions that we can reasonably investigate is 20. We thus selected 20 of the 47 test points using an exchange algorithm integrated in the NEMROD® software package[2] with the assistance of Professor Phan Tan Luu, of the experimental research laboratory at St. Jérome University in Marseille. The resulting experimentation plan is shown in Table II. The detailed glass compositions are indicated as weight percentages in Table III and as molar percentages in Table IV. The center-of-gravity composition is that of Glass IT19.

3.3 Glass Fabrication

The R7T7 reference glass and the $R7T7_{min}$ and $R7T7_{max}$ variants were prepared under the same conditions in a platinum crucible at a melting temperature of 1200°C, from phosphates, oxides and carbonates, then refined for 3 hours according to the standard laboratory procedure[36].

Certain compositions (IT12, IT13, IT15 and IT20) were modified because the glass samples exhibited segregation of the molybdic phase. We therefore diminished the Mo weight percentage in these samples, but without modifying the initial experimentation plan: the weight reduction was applied to all other oxides in the "FP & actinide oxides + ZrO_2" category to conserve this factor at its initial value in the experimentation plan.

4. INITIAL GLASS DISSOLUTION RATE AT 90°C (SA/V = 0.1 cm^{-1})

4.1 Introduction

The objective of these experiments was to identify the dissolution mechanisms under conditions far removed from saturation, and to determine the initial dissolution rates at 90°C without imposing an initial pH value.

4.2 Experimental Protocol

The Teflon® experimental leaching cells contained one liter of solution continuously stirred in an oven at 90°C. Glass coupons were prepared with a mean surface area of 13 cm^2, estimated geometrically by considering the coupons as perfect rectangular prisms. The glass monoliths were placed on Teflon® baskets.

The deionized water volume in each experimental cell was adjusted to obtain the specified glass-surface-area-to-solution-volume (SA/V) ratio. The SA/V ratio and the duration of the leach test was adjusted according to the glass composition; for most of the glass samples, the SA/V ratio was 0.1 cm^{-1} and the test lasted 6 days, with two solution samples taken per day during the first three days, and a final sample on the sixth day. Five glass compositions were exceptions to this rule, however, either because of their excessive solubility (IT5, IT13) or their high resistance (IT1, IT6, IT11). The experimental conditions under which the initial dissolution rates were measured for these five samples are indicated in Table V.

For each test, solution samples were taken from the same *Savillex* cell at 90°C. The pH was not imposed, and varied freely with the alteration solution chemistry at equilibrium with the glass. The solution pH was measured to within 0.05 pH unit at 90°C before each sample was taken, using a *Metrohm 632* pH-meter with a *Ross* Orion 8103 combined electrode.

4.3 Alteration Solution Sample Analysis

Sample aliquots were filtered to 0.45 µm and acidified to 10% with 14N HNO_3 prior to inductively-coupled plasma atomic emission spectrometry (ICP-AES) analysis using an *Yvon Jobin 70P* spectrometer analyzer coupled with a *Durr* plasma torch. The elements determined were Si, B, Na, Li, Mo, Al, Ca, Sr and Zn, with a mean analytical precision of about 3.5%; the measured concentrations $C(i)$ were corrected for the acid dilution.

The elemental normalized mass losses $NL(i)$ for each glass component element determined in solution were calculated from the corrected concentrations as follows:

$$NL(i) = \frac{C(i) \times f}{ox\%(i) \times \frac{SA}{V}}$$

where $NL(i)$ is the elemental normalized mass loss ($g \cdot m^{-2}$); $C(i)$ is the concentration ($mg \cdot l^{-1}$) of element i; f is the element/oxide conversion factor; $ox\%(i)$ is the weight percentage of oxide i in the glass; and SA/V is the glass surface-area-to-solution-volume ratio (cm^{-1}).

Dissolution rate calculation. The glass dissolution rate was calculated by linear regression over time for NL(B), NL(Na), NL(Li), NL(Mo) and NL(Si).

Rate calculation error. The errors on the initial dissolution rate calculation r_0 for Na, B, Li and Mo were estimated from the standard error s multiplied by a coefficient t following Student's law for $\nu = n-1$ degrees of freedom, where s is the number of "time | $NL(i)$" measurement pairs. The bounds on the confidence interval for the initial dissolution rate r_0 are therefore[37]:

$$r_0 \pm \frac{s}{\sqrt{n}} t_{1-\alpha/2}$$

where n ranges from 3 to 8 (95% probability level).

Congruence ratio calculation. The B/Si, Na/Si, Al/Si and Ca/Si concentration ratios in solution, corrected for dilution, were calculated and compared with the same concentration ratios in the glass. Leaching was congruent when the ratios were identical in the glass and in the leaching solution; otherwise, leaching was either selective or incongruent.

4.4 Leach Testing Results

The leach testing results (pH and normalized mass losses) are indicated in Table VI to Table XXVIII.

4.4.1 Dissolution Mechanisms

Table XXIX summarizes the dissolution conditions observed during the initial dissolution of the 23 glass samples. Two major types of dissolution were observed[38]:

- Congruent (stoichiometric) dissolution.
  - All the elements were released from the glass in the same proportions as their percentage in the initial glass composition. This type of dissolution is designated **C** in the table.
- Incongruent dissolution.
  - Certain elements *X* were released preferentially from the glass: the X/Si concentration ratio in solution was higher than in the glass. This type of incongruence is designated I(+;*d*) in the table, where *d* is the duration of the incongruence in days.
  - Some elements *X* were retained in the alteration film: the X/Si concentration ratio in solution was lower than in the glass. This type of incongruence is designated I(–;*d*) in the table, where *d* is the duration of the incongruence in days.

Boron and sodium generally exhibited the same behavior, and were released into solution at the same rate – often higher than the rate for the other elements.

Aluminum, like calcium and the metallic elements, were found in low concentrations in solution, as they were incorporated in the alteration film.

Lithium and molybdenum showed intermediate behavior, although they more closely resembled the mobile elements (B and Na).

4.4.2 Initial Dissolution Rate at 90°C: Discussion

Table XXX indicates the initial dissolution rates calculated from the normalized mass loss values for Si, B, Na, Li and Mo, together with the time period over which the dissolution rate was calculated and the mean pH.

When the 23 r_0(B) values are positioned with respect to glass composition IT19 (the reference glass in composition range "B" because its composition is the center of gravity of the experimental domain), two major classes of glass composition are discriminated by their leaching resistance:

- Group 1: high resistance, i.e. with initial dissolution rates at 90°C lower than that of IT19 (1.89 $g \cdot m^{-2} d^{-1}$). In order of decreasing durability, these compositions are the following:
  IT6 > R7T7 > IT1 > IT11 > IT7 > R7T7$_{min}$ > IT15 > IT3 > IT16 > IT18
- Group 2: low resistance, i.e. with initial dissolution rates at 90°C higher than that of IT19 (1.89 $g \cdot m^{-2} d^{-1}$) . In order of decreasing durability, these compositions are the following:
  IT19 > IT4 > R7T7$_{max}$ > IT12 > IT14 > IT17 > IT8 > IT10 > IT2 > IT20 > IT9 > IT5 > IT13

Group 1 includes glass compositions with either 20% Al_2O_3 or over 50% SiO_2. In Group 2, two samples differ substantially from the others by their extremely high dissolution rates: IT5 and IT13.

The experimental dissolution rate data can be correlated with certain aspects of the glass compositions; for example: the higher the silica and alumina concentrations, the lower the r_0(B) value (refer to Figure 1). Some exceptions to this rule were observed:

- IT2, for example, had one of the highest ($SiO_2 + Al_2O_3$) molar percentages, and would have been expected to exhibit satisfactory chemical durability. In fact, it was one of the least durable samples in Group 2. This could be attributable to its high B_2O3 content (boron has the particularity of being a three- or four-coordinate atom depending on the molar percentage of alkali metals compared with the molar percentage of SiO_2 and Al_2O_3)[17,18,19].
- IT14, with a ($SiO_2 + Al_2O_3$) molar percentage similar to that of IT5, should have exhibited a very high initial dissolution rate. For IT5, r_0(B) was 17.8 $g \cdot m^{-2} d^{-1}$, while r_0(B) was only 3.47 $g \cdot m^{-2} d^{-1}$ for IT14. This glass contained 25% fission product oxides, actinide oxides and ZrO_2 (compared with only 5% for IT5), which may have enhanced its durability. The only other notable difference

between the two glass compositions was the higher alkali metal content of IT5 (24 wt% versus 9 wt% for IT14).

- IT12, with a ($SiO_2 + Al_2O_3$) molar percentage similar to that of IT13, was much more durable: the initial dissolution rate at 90°C was 3.1 $g \cdot m^{-2} d^{-1}$ compared with 94 $g \cdot m^{-2} d^{-1}$ for IT13. The only significant differences in the compositions of these two samples were the weight percentages of B_2O_3 (7% for IT12, 20% for IT13) and the additive oxides (10% for IT12, 2.5% for IT13).

The 23 glass compositions may also be classified according to the ratio between the ($SiO_2 + Al_2O_3$) molar percentages and the sum of the network modifiers ($Na_2O + Li_2O$) and the network former B_2O_3. In decreasing order, the result is the following:

$$IT1 > IT6 > IT11 > IT15 > IT16 > R7T7_{min} > IT2 > R7T7 >$$
$$IT3 > IT19 > IT7 > IT18 > R7T7_{max} > IT8 > IT4 > IT17 >$$
$$IT10 > IT20 > IT14 > IT12 > IT9 > IT5 > IT13$$

The higher the (B_2O_3+Na_2O+Li_2O) / (SiO_2+Al_2O_3) molar ratio, the higher the initial dissolution rate (Figure 2), with one exception: IT2, as above.

4.5 Analyzing the Results with the Experimentation Plan

4.5.1 Experimentation Plan Methodology

The methodology addressed two essential questions:

1. Can the initial dissolution rate $r_0(B)$ be modeled as a function of the oxide weight percentages (SiO_2, Al_2O_3, B_2O_3, Na_2O+Li_2O, additive oxides, fission product and actinide oxides + ZrO_2)?
2. What are the effects of these six oxide groups on the initial dissolution rate at 90°C?

4.5.1.1 The Model

The objective was to represent the variations of the response Y as a function of variations in the test factors X_i selected for the study:

$$Y = f(X_1, X_2, X_3, \ldots, X_i, X_k) + e$$

where Y is the response, X_i are the factors, e is the experimental error (noise) and f is the response function. In the absence of a theoretical model, the experimenter must postulate an empirical model; the choice of a model is difficult, and is based on two "adventurous" assumptions:

- the phenomenon is continuous over the entire experimental domain;
- the response function is not complex, without a local minimum and maximum.

Under these conditions, a polynomial model is appropriate, provided the polynomial degree is sufficiently high and/or the experimental domain is sufficiently limited. The problem is thus to choose the degree and the experimental domain[39].

We selected a truncated second-degree model including only squares involving SiO_2:

$$\begin{aligned} Y = {} & b_1 \times (SiO_2) + b_2 \times (Al_2O_3) + b_3 \times (B_2O_3) + b_4 \times (Na_2O + Li_2O) + b_5 \times (\text{additive oxides}) + \\ & b_6 \times (\text{FP \& actinide oxides} + ZrO_2) + b_{12} \times (SiO_2 \times Al_2O_3) + b_{13} \times (SiO_2 \times B_2O_3) + \\ & b_{14} \times (SiO_2 \times (Na_2O + Li_2O)) + b_{15} \times (SiO_2 \times \text{additive oxides}) + \\ & b_{16} \times (SiO_2 \times (\text{FP \& actinide oxides} + ZrO_2)). \end{aligned}$$

A multilinear regression program (NEMROD®) based on the least squares criterion was used to calculate the b_1, b_2, b_3, b_4, b_5, b_6, b_{12}, b_{13}, b_{14}, b_{15} and b_{16} coefficients from the $r_0(B)$ data. The polynomial model relating $r_0(B)$, in $g \cdot m^{-2} d^{-1}$, to the weight percentages of the six selected oxide groups was the following:

$$r_0(B) = 1.81 \times (SiO_2) - 7.56 \times (Al_2O_3) + 1.22 \times (B_2O_3) + 69.14 \times (Na_2O + Li_2O) - 41.39 \times (\text{additive oxides}) + 5.35 \times (\text{FP \& actinide oxides} + ZrO_2) - 5.35 \times (SiO_2 \times Al_2O_3) + 40.91 \times (SiO_2 \times B_2O_3) - 127.67 \times (SiO_2 \times (Na_2O + Li_2O)) + 50.48 \times (SiO_2 \times \text{additive oxides}) - 27.23 \times (SiO_2 \times (\text{FP \& actinide oxides} + ZrO_2)).$$

The variance analysis for $r_0(B)$ is indicated in Table XXXI.

The experimental variance was estimated at 1.54. The result (100%) of Snedecor's test on the ratio of the validity mean square to the error mean square indicates that the model satisfactorily accounts for the measured initial dissolution rate based on the normalized boron mass loss. Similarly, the 21.5% significance for Snedecor's test applied to the ratio of the regression mean square to the error mean square shows that the model is useful, i.e. that it yields dissolution rates for which the differences between glass compositions are more significant than the experimental variance.

For the $r_0(B)$ model, $\sigma^2 = 1.24$, $R^2 = 0.86$, and $R^2_a = 0.67$.

4.5.1.2 Testing the Model

The model was tested against the experimental data acquired during prior investigations. The $r_0(B)$ values were calculated using the model equations for nine glass compositions:

- $R7T7_{max}$, $R7T7_{min}$, R7T7
- $R7T7_{-10\%}$, $R7T7_{+5\%}$, $R7T7_{+10\%}$, $R7T7_{+15\%}$, $R7T7_{4\%Mo}$, M7.

Most of the compositions in the second group are R7T7 glass samples in which the SiO_2 content was modified with respect to the nominal R7T7 composition[38]. $R7T7_{4\%Mo}$ contains 4 wt% MoO_3[40] and M7 is a less siliceous glass richer in sodium than R7T7[41]. The weight percentages of the major oxides are indicated in Table XXXII.

It should be noted that the model assumes a fixed CaO concentration of 4 wt%, but that none of these glass compositions corresponds precisely to that figure; the difference reached 27% in one case ($R7T7_{+15\%}$).

Table XXXIII compares the measured and calculated $r_0(B)$ values for all 29 glass compositions, as well as the statistical residues (i.e. the differences between the measured and calculated values). Several groups may be discriminated on the basis of the residues:

- Glasses with very high residues, i.e. an absolute value exceeding 3 $g \cdot m^{-2} d^{-1}$ (about twice the standard deviation of the experimental error): IT5, IT13.
- Glasses for which the absolute value of the residue lies between 1.24 and 3 $g \cdot m^{-2} d^{-1}$ (the estimated standard deviation of the experimental error): IT9, IT12, IT16, IT18, R7T7, $R7T7_{-10\%}$, $R7T7_{4\%Mo}$, M7.

The high residues obtained for $R7T7_{-10\%}$, $R7T7_{4\%Mo}$ and M7 glass may be attributable to the CaO concentration, which was assumed by the model to be 4 wt%. The very low initial dissolution rate of R7T7 glass remains unaccounted for.

Similarly, it is difficult to explain the high residues obtained for the other six glass compositions from the experimentation plan: IT5, IT13, IT9, IT12, IT16 and IT18. All these glasses contained 30% SiO_2 except IT5 (35% SiO_2), and three of the six contained over 20% B_2O_3 (IT9, IT5, IT13); the model largely underestimates the initial rate for the latter category. Moreover, IT9 and IT12 were identified during the comparison of the glass structure and durability (cf. § 4.4.2) as compositions that should have exhibited much higher dissolution rates – if not the highest of all – because of their low $(SiO_2+Al_2O_3) / (Na_2O+Li_2O+B_2O_3)$ ratios.

For the nineteen other glass compositions, the residue was comparable to the standard deviation: the model may thus be considered valid over the experimental range.

• *Oxide Effects*

The effects of the oxide components were plotted according to Piepel's hypotheses[42,43] using the empirical model discussed above. In this type of plot for a given model, there is one effect curve per oxide in the mixture. Each effect curve indicates how the rate predicted by the model varies as the relevant component oxide percentage varies over its composition range. The oxide effects on r_0(B) are plotted in Figure 3 for SiO_2, Al_2O_3, Na_2O+Li_2O, B_2O_3, additive oxides (AO), fission product and actinide oxides (FPO). Three observations may be made concerning the plot:

- The glass durability is increased by silica, the additive oxides (Fe, Ni, Cr, P) and by alumina.
- The fission product oxides do not appear to have a significant effect on the glass durability.
- Boron and especially the alkali metals considerably diminish the leaching resistance of borosilicate glass.

The **additive oxides** occupy positions within the glass structure that are not well known. On the basis of the experimental data, however, they are not detrimental to the glass durability. Most additive oxides are metals in solution as multivalent ions. In simple sodium silicate or borosilicate glasses, these multivalent ions (Zn^{2+}, Ni^{2+}, Cr^{3+}, Fe^{2+}, Fe^{3+}) in solution inhibit the initial stages of dissolution[44,45,46].

Silica is known to be a glass network forming oxide[24,25]; as the SiO_2 content increases, the glass becomes increasingly rigid.

Conversely, the **alkali metals** disrupt the silicate network by forming nonbridging oxygen atoms, which constitute weak points in the glass attacked by protons in the alteration solution. **Sodium** atoms may also help to ensure the electrical equilibrium of the $[AlO_4]^-$ and $[BO_4]^-$ tetrahedrons, and are thus not bonded to an oxygen atom.

Boron may be found in both 3-coordinate and 4-coordinate form in the glass[25,26]. A geometric approach is necessary to assess the network rigidity provided by 3- or 4-coordinate boron: 3-coordinate boron may be considered as a triangle, the vertices of which are bonded to the siliceous network; inserting a plane figure into a siliceous tetrahedral network breaks the sequence of $[SiO_2]$ tetrahedrons. In addition, the B–O bond is ionic, while the stronger Si–O bond is covalent. Consequently, any BO_3 triangle in the siliceous network is a structural weak point subject to preferential attack by OH^- and H^+ ions in the alteration solution. Conversely, the $[BO_4]^-$ tetrahedron may be conceived of as better integrated into a tetrahedral siliceous network. Each $[BO_4]^-$ group also requires an alkali metal atom for its valence equilibrium, thus effectively making the alkali metal atom unavailable for the destruction of the siliceous network[47,48,49]. The $[BO_4]^-$ tetrahedron therefore does not disrupt the network; the structure is not weakened, but rather reinforced or reticulated, as the number of bonds increases from 3 to 4.

Aluminum is considered in the glassmaking industry as an intermediate element: it is either a network former (4-coordinate Al) or a network modifier (6-coordinate Al).

The addition of aluminum to a SiO_2-Na_2O melt strengthens the siliceous network, but the resulting Al–Na bond is much weaker than the ionic Si–O–Na bond. Aluminum thus increases the mobility of the alkali metals during corrosion by bonding them less cohesively to the siliceous network (Figure 4). This effect has been demonstrated in SiO_2-Al_2O_3-Na_2O melts, but is mitigated in quaternary (SiO_2-Al_2O_3-B_2O_3-Na_2O) glasses and to an even greater extent in aluminoborosilicate glass compositions for fission product containment. Adding aluminum to a SiO_2-Al_2O_3-Na_2O melt enhances the glass homogeneity by eliminating segregation phenomena. But what are the proportions of tetrahedral and octahedral alumina in the 23 glass compositions investigated here?

Aluminum in tetrahedral form implies the presence of a sodium atom, as noted above. What are the consequences of this sodium consumption on the number of tetrahedral boron groups that also require sodium atoms? Studies with ternary (SiO_2-Al_2O_3-Na_2O) glass indicate that the chemical

durability of the glass increases with the number of tetrahedral (N4) boron groups; does the number of N4 boron groups diminish when alumina is present? what is the effect of a high alumina concentration on this partition?

5. GLASS DISSOLUTION RATE AT 90°C (SA/V = 200 cm^{-1})

Experiments were conducted at 90°C with an SA/V ratio of 200 cm^{-1} to determine the glass corrosion rates under conditions near saturation equilibrium. The experimental protocol was based on the MCC-1 procedure, using *Savillex*® Teflon® (PTFE) containers with a 7 ml unit volume. Two grams of glass powder with a grain size of 40–50 µm were placed in contact with 5 ml of initially pure water to obtain an SA/V ratio of 200 cm^{-1}. The SA/V ratio and the test duration schedule were identical for all the glass compositions tested.

The containers were inserted into sealed glass tubes containing a few milliliters of water to minimize water losses; the tubes were placed in an oven maintained at a constant temperature of 90°C ± 1°C. Test durations of 14, 28, 56, 91, 119 and 182 days were scheduled, and each glass was tested in triplicate for each duration. Each alteration solution sample was ultrafiltered to 18 Å before ICP-AES analysis to determine the following elements: Si, B, Na, Li, Al, Zn, Fe, Zr, Ca and Nd.

The main test results are summarized in Table XXXIV. The glass compositions are listed in order of increasing normalized boron mass loss after 182 days; other information in the table includes the corrosion rates calculated by linear regression between 28 and 182 days for the test SA/V ratio (200 cm^{-1}), the corresponding initial corrosion rate measured at a low SA/V ratio (0.1 cm^{-1}), the Si and H_4SiO_4 concentrations, the glass molecular weight, and the final solution pH.

All the orthosilicic acid activity values have not been calculated as of this writing. These values should indicate whether silica is the only critical element in controlling the glass corrosion kinetics, as the SiO_2 concentrations in the test matrices were highly variable. The results will be provided in the next report, and discussed with reference to the LIXIVER model[49].

Several remarks may be made concerning Table XXXIV:

- The normalized mass losses for the least durable glass (IT4) and the most durable glass (IT15) differ by a factor of 232 (column 2).
- The lowest final corrosion rate (IT6: 0.008×10^{-2} $g \cdot m^{-2} d^{-1}$) and the highest final rates (IT9: 9.5×10^{-2} $g \cdot m^{-2} d^{-1}$, and R7T7$_{min}$: 9.9×10^{-2} $g \cdot m^{-2} d^{-1}$) differed by a factor of 1000 (the corrosion rate for the R7T7 reference glass between 28 and 182 days was 0.8×10^{-2} $g \cdot m^{-2} d^{-1}$).
- The glass compositions with the lowest initial corrosion rates (column 4) were not necessarily those with the lowest final corrosion rates (column 3) or the lowest normalized boron mass losses after 182 days of alteration (column 2) at an SA/V ratio of 200 cm^{-1} (cf. IT11 and IT6).
- Conversely, the glass compositions with initial corrosion rates significantly higher than R7T7 glass did not necessarily have high final corrosion rates or high long-term normalized mass losses (cf. IT19, IT18, 1T2 and IT14).
- The most soluble glass compositions yielded high solution pH values (column 8) with some exceptions: IT19 was relatively insoluble, but the final pH was 10.1; IT10 and IT11 were quite soluble, but had final pH values of 9.5 and 9.8, respectively.
- There was no correlation between the silica concentration in solution (column 5) and the total dissolved glass quantity (column 2).
- Unlike the results observed for the initial dissolution rates, there was no correlation between the final corrosion rate r_f and the concentration of network formers ($SiO_2 + Al_2O_3$) in the glass (Figure 1).
- There was no correlation between the $(Na_2O + Li_2O + B_2O_3) / (SiO_2 + Al_2O_3)$ molar ratio in the glass and the normalized boron mass loss after 182 days (Figure 2), nor between this molar ratio and the final corrosion rates.

At the present stage of this investigation, it is impossible to predict the effects of the glass composition on the long-term behavior. Corrosion experiments with glass powder samples thus continue to remain the only quantitative means of estimating long-term glass stability.

6. CONCLUSIONS

Twenty aluminoborosilicate glass compositions containing simulated fission product oxides were defined using the experimentation plan methodology. Three additional glass compositions were also tested.

Monolithic glass corrosion tests in a dilute aqueous medium at 90°C indicated the variation range for the initial corrosion rates r_0. Significant but only qualitative correlations were established between the initial corrosion rate and the molar fraction of glass network forming oxides ($SiO_2 + Al_2O_3$), and between the initial rate and the $(Na_2O + Li_2O + B_2O_3) / (SiO_2 + Al_2O_3)$ molar ratio in the glass. The experimentation plan allowed a polynomial model to be defined relating the initial corrosion rate at 90°C to the oxide concentrations in the glass. Although the model is theoretically capable of predicting the corrosion rates, it does not always account for the actual data measured during other experiments; this discrepancy may be attributable either to the presence of other chemical elements (MgO) or to CaO concentrations differing from the fixed value adopted for the experimentation plan. Considering the current (partial) results obtained, the pertinence of the experimentation plan for a very wide range of glass compositions may be called into question: would it not be preferable to adopt this strategy for composition subsets specified for more limited composition ranges?

Glass powder corrosion tests designed to simulate advanced corrosion reaction progress, account for the wide variations in the dissolved glass quantities, although no correlation exists with the glass chemical composition. At the current stage of the investigation it is too early to conclude. Still unanswered questions include the role of secondary alteration products in controlling the composition of the alteration solution, and the kinetic law governing all the glass compositions tested. The partial results available at this time cast doubts on the pertinence of a rate law in which the reaction affinity is based exclusively on the orthosilicic acid activity in solution.

REFERENCES

1. A. TERKI and F. PACAUD, AFNOR data sheet.
2. Vitrified Waste Specification, AQO 16 July 1986.
3. J. GODARD, *Spécifications des verres: Analyses des tolérances de composition chimique*, CEA internal note.
4. N. JACQUET-FRANCILLON, *Standardisation des données de vitrification des solutions de référence R7T7*, CEA internal note.
5. F. PACAUD, N. JACQUET-FRANCILLON, A. Terki and C. Fillet, *Scientific Basis for Nuclear Waste Management XII*, eds. Werner LUTZE and Rodney C. EWING (Material Research Society 1989) pp. 105-120.
6. F. PACAUD, A. TERKI, C. FILLET, L. PELLEGRIN, D. RIGAUD, M. ST-GAUDENS, A. GAVAZZI and C. GUIHARD, CEA internal note.
7. A. TERKI, F. PACAUD and N. Jacquet-Francillon, CEA internal note.
8. C. FILLET, F. PACAUD, A. TERKI and N. JACQUET-FRANCILLON, CEA internal note.
9. C. FILLET, F. PACAUD, A. TERKI and N. JACQUET-FRANCILLON, .
10. I. TOVENA, T. ADVOCAT, D. GHALEB, E. VERNAZ and F. LARCHE, *Material Research Symposium Proceedings* vol. 333, pp. 595-602(1994).
11. X. FENG and A. BARKATT, *Material Research Symposium Proceedings* vol. 112, p. 543 (1988).
12. C. COMPAGNON, A. GAVAZZI, M. LEGOUX, F. PACAUD, D. RIGAUD and A. TERKI, CEA internal note .
13. S. GIN, *Etude expérimentale de l'influence d'espèces aqueuses sur la cinétique de dissolution du verre nucléaire R7T7*, PhD thesis, University of Poitiers (1994).
14. T. ABE, *J. Am. Ceram. Soc.*, vol. 35 p. 284 (1952)
15. S.P. ZHDANOV and E.V. KOROMALDI, *Proceedings of VIIth Int. Conf. on Glass*, 302 (1965)
16. P. VAN ISEGHEM, T. AMAYA, Y. SUZUKI and H. YAMAMOTO, *J. of Nucl. Mat.*, vol. 190 pp. 26-276 (1992).
17 Y.H. YUN and P.J. BRAY, *J. Non Crystalline Solids*, vol. 27, p. 363 (1978)
18 H. SCHOLTZE, *Le verre: Nature, structure et propriétés*. 2nd edition, Institut du verre, Paris (1980).
19 J. ZARZYCKI, *Les verres et l'état vitreux*, Masson, Paris (1982).
20. S.P. ZHDANOV and E.V. KOROMALDI, *The Structure of Glass*. vol. 8, ed. E.A. Porai Koshits (1973).
21. M. JEANMAIRE, *Verres Réfractaires*, vol. 24, No 1 (1970)
22. F. PACAUD, *Standardisation des données de vitrification des solutions du verre de référence R7T7*, CEA internal note.
23. X. FENG, I. PEGG, A. BARKATT, P. MACEDO and S. CUCINELL, S. LAI, *Nuclear Tech.* vol. 85 (1989).
24. J.L. NOGUES, J.P. MESTRE AND E. VERNAZ., *Effet du remplacement partiel de Na_2O par différents oxyde modificateurs sur la lixiviation à 90°C du verre R7T7 SON 68 18 17 L1C2A2Z1*, CEA internal note.
25. J.C. TAIT and D.L. MANDOLESI, *Rapport des établissements de recherche nucléaire de Whiteshell (Canada)*, AECL 7803 (1983).
26. P. VAN ISEGHEM, T. AMAYA, Y. SUZUKI and H. YAMAMOTO, *J. of Nucl. Mat.* vol. 190 pp. 269-272 (1992).
27. J. ST. PIERRE, H.H. TRAN and L. ZIKOVSKY, *J. of Nuclear Mat.*, vol. 107, pp. 286-289 (1982).
28. W. DUCAN, RANKIN and G.G. WICKS, *J. of Am. Ceram. Soc.*, vol. 66, No 6 (1983)
29. R.A. MCLEAN, V.L. ANDERSON, "Extreme vertices design of mixtures experiments", *Technometrics* vol. 23, No 2 (1981).

30. L.A. CHICK, G.F. PIEPEL, G.B. MELLINGER, R.P. MAY, W.J. GRAY and C.Q. BUUWALKER, PNL 3188 UC70.
31. L.A CHICK and G.F. PIEPEL, *J. of Am. Ceram Soc.*, vol. 967 No 11 (1984).
32. G.F. PIEPEL, .B. MELLINGER and M.A.H. REIMUS, *Waste Management*, vol. 9. pp. 3-11 (1989).
33. P. ARMA, G.F. PIEPEL, M.J. SCHWEIGER and D.E. SMITH, PNL SA-20362 (1992)
34. P.D. SOPER, D. WALKER, M.J. PLODINEC, G.J. ROBERTS and C.F. LIGHTNER, *Ceramic Bulletin*, vol. 62 No 9 (1983).
35. G.F. PIEPEL, P.P. ARMA, S.O. BATS, M.J. SCHWEIGER and D.E. SMITH, *First Order Study of Property/Composition Relationships for Hanford Waste Vitrification Plant Glasses*, PNL 8502-UC 721.
36. F. PACAUD and C. Fillet, *Préparation des verres inactifs en creuset de platine: I. Méthode classique: Mode opératoire*, CEA internal note.
37. M. NEUILLY, *Modélisation: Estimation des erreurs de mesure*, Cetama, Tech. Doc. (1993)
38. T. ADVOCAT, P. JOLLIVET, N. GODON and E. VERNAZ, *Effect of Geological Repository Parameters on Aqueous Corrosion of Nuclear Glass*, CEC Contract FI 2W CT 90 0027, 1991 Annual report, CEA document.
39. G.E.P. BOX and N.R. DRAPER, "A Basis for the Selection of a Response Surface Design", *J. Am. Statis. Assoc.*, 54, 62-654 (1959).
40. T. ADVOCAT and J.L. CHOUCHAN, *Etude de la corrosion aqueuse du composé vitrocrystallin SPNM: comportement à long terme*, CEA internal note.
41. T. ADVOCAT, N. GODON, P. JOLLIVET, E. VERNAZ and F. DELAGE, *Corrosion aqueuse des verres nucléaires. Influence des conditions de stockage. Incorporation de MgO aux verres R7T7 et M7*, CEC contract FI 2WCT900027. Annual report (1991).
42. G.F. PIEPEL, "Component Effects in Mixture Experiments". *Proc. of Dept. of Energy Statistical Symposium*, Gattimburg, Tennessee, (1979).
43. G.F. PIEPEL, "Measuring Component Effects in Constrained Mixtures", *Technometrics* 24, 29-39 (1982).
44. M.F. DILMORE *Chemical Durability of Multicomponent Silicate Glasses*, PhD Thesis, University of Florida (1977).
45. J.C. TAIT and C.D. JENSEN, "The Effect of Zn(II) Ion Adsorption on the Durability of Sodium Borosilicate Glasses", *J. of Non Cryst. Solids*, 49, 363 (1982)
46. P. MAYER, J.A. TOPPING and J.L. LACKNER, "Effect of Additions of Transition Metal Oxides on the Corrosion Kinetics of a K_2O-Na_2O-BaO-SiO_2 Glass in Aqueous KOH Solutions", *J. Amer. Ceram. Soc.*, 60, 181 (1977)
47. B.M.J. SMETZ and T.P. MLOMMEN "The Leaching of Sodium Aluminosilicate Glasses Studied by Secondary Ion Mass Spectrometry", *Phys. Chem. Glasses*, 23, 83 (1982)
48. K. KOBAYASH and H. OKUMA, "^{11}B and ^{27}Al Nuclear Quadrupole Interactions in SiO_2-B_2O_3-Al_2O_3-R_2O Glass Systems", *J. Am. Ceram. Soc.*, 59 354 (1976)
49. P. JOLLIVET, F. DELAGE, T. ADVOCAT, N. GODON and E. VERNAZ, CEC contract FI2WCT90 (1993).

LIST OF TABLES

Table I. Composition of R7T7 glass and variants (oxide wt%), with characteristic temperature values

Oxides	$R7T7_{min}$	R7T7	$R7T7_{max}$
SiO_2	51.70	45.48	42.40
Al_2O_3	6.60	4.91	3.60
B_2O_3	12.40	14.02	16.50
Na_2O	8.10	9.86	11.00
Li_2O	1.60	1.98	2.40
CaO	3.50	4.04	4.80
Fe_2O_3	0.00	2.91	4.50
NiO	0.39	0.74	0.79
Cr_2O_3	0.20	0.51	0.20
ZnO	2.20	2.50	2.80
P_2O_5	1.00	0.28	0.00
ZrO_2	3.45	2.65	1.97
SrO	0.29	0.33	0.29
Y_2O_3	0.18	0.20	0.18
MoO_3	1.49	1.70	1.52
MnO_2	0.63	0.72	0.64
CoO	0.11	0.12	0.11
Ag_2O	0.30	0.03	0.03
CdO	0.03	0.03	0.03
SnO_2	0.02	0.02	0.02
Sb_2O_3	0.01	0.01	0.01
TeO_2	0.20	0.23	0.21
Cs_2O	1.24	1.42	1.27
BaO	0.53	0.60	0.54
La_2O_3	0.79	0.90	0.80
Ce_2O_3	0.81	0.93	0.83
Pr_2O_3	0.39	0.44	0.39
Nd_2O_3	1.39	1.59	1.42
UO_2	0.46	0.52	0.46
ThO_2	0.29	0.33	0.30
Transition point Tg (°C)	531	505	475
Annealing point (°C)	520	520	520
Melting point (°C)	1200	1200	1200

Table II. Composition of 20 glass samples (oxide wt%), with characteristic temperature values

Glass	SiO_2	Al_2O_3	B_2O_3	Na_2O	Li_2O	CaO	Additive oxides	(FP+Act +Zr) oxides	Tg (°C)	$T_{elaboration}$ (°C)
IT1	70.00	2.00	7.00	7.47	1.53	4.00	3.00	5.00	521	1350
IT2	57.50	2.00	20.00	7.47	1.53	4.00	2.50	5.00	522	1200
IT3	55.50	2.00	7.00	19.92	4.08	4.00	2.50	5.00	440	1200
IT4	48.00	2.00	7.00	19.92	4.08	4.00	10.00	5.00	425	1100
IT5	35.00	2.00	20.00	19.92	4.08	4.00	10.00	5.00	430	1100
IT6	52.50	20.00	7.00	7.47	1.53	4.00	2.50	5.00	572	1375
IT7	32.00	20.00	20.00	7.47	1.53	4.00	10.00	5.00	515	1300
IT8	37.50	20.00	7.00	19.92	4.08	4.00	2.50	5.00	424	1200
IT9	30.00	14.50	20.00	19.92	4.08	4.00	2.50	5.00	428	1200
IT10	30.00	20.00	7.00	19.92	4.08	4.00	10.00	5.00	428	1200
IT11	50.50	2.00	7.00	7.47	1.53	4.00	2.50	25.00	530	1300
IT12	30.00	2.00	7.00	18.26	3.74	4.00	10.00	25.00	455	1200
IT13	30.00	2.00	20.00	19.92	4.08	4.00	2.50	17.50	429	950
IT14	30.00	2.00	20.00	7.47	1.53	4.00	10.00	25.00	505	1100
IT15	32.50	20.00	7.00	7.47	1.53	4.00	2.50	25.00	561	1375
IT16	30.00	20.00	7.00	7.47	1.53	4.00	10.00	20.00	528	1375
IT17	30.00	9.50	20.00	7.47	1.53	4.00	2.50	25.00	518	1100
IT18	30.00	20.00	20.00	7.47	1.53	4.00	2.50	14.50	515	1300
IT19	39.30	9.60	12.40	12.70	2.60	4.00	5.80	13.60	482	1200
IT20	30.00	13.70	7.00	19.92	4.08	4.00	2.50	18.80	428	1200

Table III. Detailed composition of glass samples (oxide wt%)

Glass	SiO_2	Al_2O_3	B_2O_3	Na_2O	Li_2O	CaO	Fe_2O_3	NiO	Cr_2O_3	ZnO	P_2O_5	ZrO_2	SrO	Y_2O_3	MoO_3	MnO_2	CoO	Ag_2O	CdO	SnO_2	Sb_2O_3	TeO_2	Cs_2O	BaO	La_2O_3	Ce_2O_3	Pr_2O_3	Nd_2O_3	UO_2	ThO_2
1	70.00	2.00	7.00	7.47	1.53	4.00	1.26	0.32	0.22	1.08	0.12	1.04	0.13	0.08	0.67	0.28	0.05	0.01	0.01	0.01	0.00	0.09	0.56	0.23	0.35	0.36	0.17	0.62	0.20	0.13
2	57.50	2.00	20.00	7.47	1.53	4.00	1.05	0.27	0.18	0.90	0.10	1.04	0.13	0.08	0.67	0.28	0.05	0.01	0.01	0.01	0.00	0.09	0.56	0.23	0.35	0.36	0.17	0.62	0.20	0.13
3	55.50	2.00	7.00	19.92	4.08	4.00	1.05	0.27	0.18	0.90	0.10	1.04	0.13	0.08	0.67	0.28	0.05	0.01	0.01	0.01	0.00	0.09	0.56	0.23	0.35	0.36	0.17	0.62	0.20	0.13
4	48.00	2.00	7.00	19.92	4.08	4.00	4.19	1.07	0.74	3.60	0.40	1.04	0.13	0.08	0.67	0.28	0.05	0.01	0.01	0.01	0.00	0.09	0.56	0.23	0.35	0.36	0.17	0.62	0.20	0.13
5	35.00	2.00	20.00	19.92	4.08	4.00	4.19	1.07	0.74	3.60	0.40	1.04	0.13	0.08	0.67	0.28	0.05	0.01	0.01	0.01	0.00	0.09	0.56	0.23	0.35	0.36	0.17	0.62	0.20	0.13
6	52.50	20.00	7.00	7.47	1.53	4.00	1.05	0.27	0.18	0.90	0.10	1.04	0.13	0.08	0.67	0.28	0.05	0.01	0.01	0.01	0.00	0.09	0.56	0.23	0.35	0.36	0.17	0.62	0.20	0.13
7	32.00	20.00	20.00	7.47	1.53	4.00	4.19	1.07	0.74	3.60	0.40	1.04	0.13	0.08	0.67	0.28	0.05	0.01	0.01	0.01	0.00	0.09	0.56	0.23	0.35	0.36	0.17	0.62	0.20	0.13
8	37.50	20.00	7.00	19.92	4.08	4.00	1.05	0.27	0.18	0.90	0.10	1.04	0.13	0.08	0.67	0.28	0.05	0.01	0.01	0.01	0.00	0.09	0.56	0.23	0.35	0.36	0.17	0.62	0.20	0.13
9	30.00	14.50	20.00	19.92	4.08	4.00	1.05	0.27	0.18	0.90	0.10	1.04	0.13	0.08	0.67	0.28	0.05	0.01	0.01	0.01	0.00	0.09	0.56	0.23	0.35	0.36	0.17	0.62	0.20	0.13
10	30.00	20.00	7.00	19.92	4.08	4.00	4.19	1.07	0.74	3.60	0.40	1.04	0.13	0.08	0.67	0.28	0.05	0.01	0.01	0.01	0.00	0.09	0.56	0.23	0.35	0.36	0.17	0.62	0.20	0.13
11	50.50	2.00	7.00	7.47	1.53	4.00	1.05	0.27	0.18	0.90	0.10	5.19	0.65	0.39	3.33	1.41	0.23	0.06	0.06	0.04	0.02	0.45	2.78	1.17	1.76	1.82	0.86	3.11	1.02	0.65
12	30.00	2.00	7.00	18.26	3.74	4.00	4.19	1.07	0.74	3.60	0.40	5.97	0.75	0.45	0.00	1.63	0.27	0.07	0.07	0.05	0.02	0.52	3.21	1.36	2.03	2.10	0.99	3.59	1.17	0.75
13	30.00	2.00	20.00	19.92	4.08	4.00	1.05	0.27	0.18	0.90	0.10	4.03	0.50	0.30	0.65	1.10	0.18	0.05	0.05	0.03	0.02	0.35	2.16	0.91	1.37	1.42	0.67	2.42	0.79	0.50
14	30.00	2.00	20.00	7.47	1.53	4.00	4.19	1.07	0.74	3.60	0.40	5.19	0.65	0.39	3.33	1.41	0.24	0.06	0.06	0.04	0.02	0.45	2.78	1.17	1.76	1.82	0.86	3.11	1.02	0.65
15	32.50	20.00	7.00	7.47	1.53	4.00	1.05	0.27	0.18	0.90	0.10	5.67	0.71	0.43	1.30	1.54	0.26	0.07	0.07	0.04	0.02	0.49	3.04	1.29	1.93	1.99	0.94	3.40	1.11	0.71
16	30.00	20.00	7.00	7.47	1.53	4.00	4.19	1.07	0.74	3.60	0.40	4.15	0.52	0.31	2.66	1.13	0.19	0.05	0.05	0.03	0.02	0.36	2.22	0.94	1.41	1.46	0.69	2.49	0.81	0.52
17	30.00	9.50	20.00	7.47	1.53	4.00	1.05	0.27	0.18	0.90	0.10	5.19	0.65	0.39	3.33	1.41	0.24	0.06	0.06	0.04	0.02	0.45	2.78	1.17	1.76	1.82	0.86	3.11	1.02	0.65
18	30.00	20.00	20.00	7.47	1.53	4.00	1.05	0.27	0.18	0.90	0.10	3.01	0.37	0.23	1.93	0.82	0.14	0.03	0.03	0.02	0.01	0.26	1.61	0.68	1.02	1.06	0.50	1.81	0.59	0.37
19	39.30	9.60	12.40	12.70	2.60	4.00	2.43	0.62	0.43	2.09	0.23	2.82	0.35	0.21	1.81	0.77	0.13	0.03	0.03	0.02	0.01	0.24	1.51	0.64	0.96	0.99	0.47	1.69	0.55	0.35
20	30.00	13.70	7.00	19.92	4.08	4.00	1.05	0.27	0.18	0.90	0.10	4.26	0.53	0.32	1.02	1.16	0.19	0.05	0.05	0.03	0.02	0.37	2.28	0.96	1.45	1.49	0.71	2.55	0.84	0.53
$r_0$max	42.40	3.60	16.50	11.00	2.40	4.80	4.50	0.79	0.20	2.80	0.00	1.97	0.29	0.18	1.52	0.64	0.11	0.03	0.03	0.02	0.01	0.21	1.27	0.54	0.80	0.83	0.39	1.42	0.46	0.30
$r_0$min	51.70	6.60	12.40	8.10	1.60	3.50	0.00	0.39	0.20	2.20	1.00	3.45	0.29	0.18	1.49	0.63	0.11	0.03	0.03	0.02	0.01	0.20	1.24	0.53	0.79	0.81	0.39	1.39	0.46	0.29
R7T7	45.48	4.91	14.02	9.86	1.98	4.04	2.91	0.74	0.51	2.50	0.28	2.65	0.33	0.20	1.70	0.72	0.12	0.03	0.03	0.02	0.01	0.23	1.42	0.60	0.90	0.93	0.44	1.59	0.52	0.33

Table IV. Detailed composition of glass samples (molar percentages)

Glass	SiO_2	Al_2O_3	B_2O_3	Na_2O	Li_2O	CaO	Fe_2O_3	NiO	Cr_2O_3	ZnO	P_2O_5	ZrO_2	SrO	Y_2O_3	MoO_3	MnO_2	CoO	Ag_2O	CdO	SnO_2	Sb_2O_3	TeO_2	Cs_2O	BaO	La_2O_3	Ce_2O_3	Pr_2O_3	Nd_2O_3	UO_2	ThO_2
1	7.35E-1	1.24E-2	6.35E-2	7.60E-2	3.24E-2	4.50E-2	4.97E-3	2.70E-3	9.14E-4	8.38E-3	5.38E-4	5.31E-3	7.87E-4	2.19E-4	2.92E-3	2.05E-3	3.96E-4	3.20E-5	5.77E-5	3.28E-5	8.47E-6	3.56E-4	1.25E-3	9.66E-4	6.83E-4	7.00E-4	3.30E-4	1.17E-3	4.76E-4	3.09E-4
2	6.14E-1	1.26E-2	1.84E-1	7.73E-2	3.29E-2	4.57E-2	4.21E-3	2.29E-3	7.77E-4	7.10E-3	4.56E-4	5.40E-3	8.00E-4	2.22E-4	2.97E-3	2.08E-3	4.02E-4	3.25E-5	5.87E-5	3.33E-5	8.61E-6	3.62E-4	1.27E-3	9.82E-4	6.94E-4	7.12E-4	3.35E-4	1.19E-3	4.84E-4	3.14E-4
3	5.68E-1	1.21E-2	6.19E-2	1.98E-1	8.42E-2	4.39E-2	4.04E-3	2.20E-3	7.45E-4	6.81E-3	4.36E-4	5.18E-3	7.67E-4	2.13E-4	2.84E-3	2.00E-3	3.86E-4	3.12E-5	5.63E-5	3.20E-5	8.26E-6	3.47E-4	1.21E-3	9.42E-4	6.66E-4	6.83E-4	3.21E-4	1.14E-3	4.64E-4	3.01E-4
4	5.09E-1	1.25E-2	6.41E-2	2.05E-1	8.72E-2	4.54E-2	1.67E-2	9.09E-3	3.08E-3	2.82E-2	1.81E-3	5.37E-3	7.95E-4	2.21E-4	2.94E-3	2.07E-3	4.00E-4	3.23E-5	5.83E-5	3.31E-5	8.55E-6	3.59E-4	1.26E-3	9.76E-4	6.89E-4	7.07E-4	3.33E-4	1.18E-3	4.80E-4	3.12E-4
5	3.78E-1	1.27E-2	1.87E-1	2.09E-1	8.89E-2	4.63E-2	1.71E-2	9.27E-3	3.14E-3	2.87E-2	1.84E-3	5.47E-3	8.10E-4	2.25E-4	3.00E-3	2.11E-3	4.07E-4	3.29E-5	5.94E-5	3.37E-5	8.72E-6	3.66E-4	1.28E-3	9.94E-4	7.02E-4	7.20E-4	3.39E-4	1.20E-3	4.89E-4	3.18E-4
6	5.96E-1	1.34E-2	6.86E-2	8.22E-2	3.50E-2	4.87E-2	4.48E-3	2.44E-3	8.26E-4	7.55E-3	4.84E-4	5.75E-3	8.51E-4	2.37E-4	3.15E-3	2.21E-3	4.28E-4	3.46E-5	6.24E-5	3.55E-5	9.16E-6	3.85E-4	1.35E-3	1.05E-3	7.38E-4	7.57E-4	3.56E-4	1.26E-3	5.14E-4	3.34E-4
7	3.86E-1	1.42E-2	2.08E-1	8.73E-2	3.72E-2	5.17E-2	1.90E-2	1.03E-2	3.50E-3	3.21E-2	2.06E-3	6.10E-3	9.04E-4	2.51E-4	3.35E-3	2.35E-3	4.55E-4	3.67E-5	6.63E-5	3.76E-5	9.73E-6	4.09E-4	1.43E-3	1.11E-3	7.84E-4	8.04E-4	3.78E-4	1.34E-3	5.46E-4	3.54E-4
8	4.16E-1	1.31E-2	6.70E-2	2.14E-1	9.12E-2	4.75E-2	4.37E-3	2.38E-3	8.06E-4	7.37E-3	4.72E-4	5.61E-3	8.30E-4	2.31E-4	3.08E-3	2.16E-3	4.18E-4	3.37E-5	6.09E-5	3.46E-5	8.94E-6	3.76E-4	1.31E-3	1.02E-3	7.20E-4	7.39E-4	3.48E-4	1.23E-3	5.02E-4	3.26E-4
9	3.31E-1	9.41E-2	1.90E-1	2.13E-1	9.07E-2	4.72E-2	4.35E-3	2.37E-3	8.02E-4	7.33E-3	4.70E-4	5.58E-3	8.26E-4	2.30E-4	3.06E-3	2.15E-3	4.15E-4	3.36E-5	6.06E-5	3.44E-5	8.89E-6	3.74E-4	1.31E-3	1.01E-3	7.16E-4	7.35E-4	3.46E-4	1.22E-3	4.99E-4	3.24E-4
10	3.45E-1	1.36E-1	6.95E-2	2.22E-1	9.47E-2	4.93E-2	1.82E-2	9.87E-3	3.34E-3	3.06E-2	1.96E-3	5.82E-3	8.62E-4	2.40E-4	3.20E-3	2.24E-3	4.34E-4	3.50E-5	6.32E-5	3.59E-5	9.28E-6	3.90E-4	1.36E-3	1.06E-3	7.48E-4	7.67E-4	3.61E-4	1.28E-3	5.21E-4	3.38E-4
11	6.14E-1	1.43E-2	7.34E-2	8.80E-2	3.75E-2	5.21E-2	4.79E-3	2.61E-3	8.84E-4	8.08E-3	5.18E-4	3.07E-2	4.55E-3	1.27E-3	1.69E-2	1.18E-2	2.29E-3	1.85E-4	3.34E-4	1.90E-4	4.90E-5	2.06E-3	7.20E-3	5.59E-3	3.95E-3	4.05E-3	1.91E-3	6.75E-3	2.75E-3	1.79E-3
12	3.72E-1	1.46E-2	7.50E-2	2.20E-1	9.36E-2	5.31E-2	1.96E-2	1.06E-2	3.60E-3	3.30E-2	2.11E-3	3.61E-2	5.40E-3	1.49E-3	0	1.40E-2	2.69E-3	2.25E-4	4.06E-4	2.47E-4	5.11E-5	2.43E-3	8.49E-3	6.61E-3	4.64E-3	4.77E-3	2.24E-3	7.95E-3	3.23E-3	2.12E-3
13	3.43E-1	1.35E-2	1.97E-1	2.21E-1	9.40E-2	4.90E-2	4.51E-3	2.45E-3	8.31E-4	7.60E-3	4.87E-4	2.25E-2	3.33E-3	9.24E-4	3.10E-3	8.66E-3	1.67E-3	1.33E-4	2.41E-4	1.37E-4	3.77E-5	1.51E-3	5.27E-3	4.09E-3	2.89E-3	2.96E-3	1.39E-3	4.94E-3	2.01E-3	1.30E-3
14	3.89E-1	1.53E-2	2.24E-1	9.38E-2	4.00E-2	5.55E-2	2.04E-2	1.11E-2	3.76E-3	3.44E-2	2.21E-3	3.28E-2	4.85E-3	1.35E-3	1.80E-2	1.26E-2	2.44E-3	1.98E-4	3.58E-4	2.01E-4	5.34E-5	2.19E-3	7.68E-3	5.96E-3	4.21E-3	4.32E-3	2.03E-3	7.20E-3	2.93E-3	1.90E-3
15	4.35E-1	1.58E-1	8.09E-2	9.69E-2	4.13E-2	5.73E-2	5.28E-3	2.87E-3	9.73E-4	8.90E-3	5.70E-4	3.70E-2	5.48E-3	1.53E-3	7.26E-3	1.43E-2	2.76E-3	2.25E-4	4.07E-4	2.29E-4	6.07E-5	2.48E-3	8.67E-3	6.73E-3	4.75E-3	4.88E-3	2.29E-3	8.13E-3	3.31E-3	2.15E-3
16	4.01E-1	1.57E-1	8.07E-2	9.67E-2	4.12E-2	5.72E-2	2.11E-2	1.15E-2	3.88E-3	3.55E-2	2.28E-3	2.70E-2	4.00E-3	1.11E-3	1.48E-2	1.04E-2	2.01E-3	1.63E-4	2.94E-4	1.65E-4	4.40E-5	1.81E-3	6.33E-3	4.92E-3	3.47E-3	3.56E-3	1.68E-3	5.94E-3	2.42E-3	1.57E-3
17	3.87E-1	7.23E-2	2.23E-1	9.35E-2	3.98E-2	5.53E-2	5.09E-3	2.77E-3	9.39E-4	8.59E-3	5.50E-4	3.27E-2	4.84E-3	1.35E-3	1.79E-2	1.26E-2	2.43E-3	1.97E-4	3.55E-4	2.01E-4	5.32E-5	2.19E-3	7.65E-3	5.94E-3	4.20E-3	4.30E-3	2.03E-3	7.17E-3	2.92E-3	1.90E-3
18	3.75E-1	1.47E-1	2.16E-1	9.05E-2	3.85E-2	5.35E-2	4.93E-3	2.68E-3	9.09E-4	8.31E-3	5.33E-4	1.83E-2	2.72E-3	7.55E-4	1.01E-2	7.06E-3	1.36E-3	1.10E-4	1.99E-4	1.15E-4	2.83E-5	1.23E-3	4.29E-3	3.33E-3	2.36E-3	2.42E-3	1.14E-3	4.03E-3	1.64E-3	1.07E-3
19	4.60E-1	6.62E-2	1.25E-1	1.44E-1	6.14E-2	5.02E-2	1.07E-2	5.82E-3	1.97E-3	1.81E-2	1.16E-3	1.61E-2	2.39E-3	6.64E-4	8.85E-3	6.21E-3	1.20E-3	9.70E-5	1.75E-4	9.81E-5	2.65E-5	1.08E-3	3.78E-3	2.93E-3	2.07E-3	2.12E-3	1.00E-3	3.54E-3	1.44E-3	9.36E-4
20	3.59E-1	9.65E-2	7.22E-2	2.31E-1	9.83E-2	5.12E-2	4.72E-3	2.57E-3	8.69E-4	7.95E-3	5.09E-4	2.48E-2	3.67E-3	1.02E-3	5.09E-3	9.56E-3	1.85E-3	1.49E-4	2.69E-4	1.53E-4	3.94E-5	1.67E-3	5.81E-3	4.51E-3	3.19E-3	3.27E-3	1.54E-3	5.45E-3	2.22E-3	1.44E-3
r0max	4.84E-1	2.42E-2	1.63E-1	1.22E-1	5.52E-2	5.87E-2	1.93E-2	7.25E-3	9.02E-4	2.36E-2	0	1.10E-2	1.92E-3	5.47E-4	7.24E-3	5.05E-3	1.01E-3	8.88E-5	1.60E-4	9.10E-5	2.35E-5	9.02E-4	3.09E-3	2.41E-3	1.68E-3	1.73E-3	8.11E-4	2.89E-3	1.17E-3	7.79E-4
r0min	5.88E-1	4.42E-2	1.22E-1	8.92E-2	3.67E-2	4.26E-2	0	3.57E-3	8.99E-4	1.85E-2	4.81E-3	1.91E-2	1.91E-3	5.45E-4	7.07E-3	4.95E-3	1.00E-3	8.84E-5	1.60E-4	9.07E-5	2.34E-5	8.56E-4	3.01E-3	2.36E-3	1.66E-3	1.69E-3	8.08E-4	2.82E-3	1.16E-3	7.50E-4
R7T7	5.25E-1	3.34E-2	1.40E-1	1.10E-1	4.61E-2	5.00E-2	1.27E-2	6.87E-3	2.33E-3	2.13E-2	1.37E-3	1.49E-2	2.21E-3	6.15E-4	8.19E-3	5.75E-3	1.11E-3	8.98E-5	1.62E-4	9.21E-5	2.38E-5	1.00E-3	3.50E-3	2.71E-3	1.92E-3	1.97E-3	9.26E-4	3.28E-3	1.34E-3	8.67E-4

Table V. Modified experimental conditions for initial dissolution rate measurements of 5 glass compositions

Glass sample	SA/V (cm^{-1})	Leaching duration (days)	Sampling schedule (days)
Highly soluble compositions			
IT5	0.1	2	3 samples per day
IT13	0.05	2	3 samples per day
Highly insoluble compositions			
IT1	0.14	3	2 samples per day
IT6	0.13	21	1, 3, 7, 14, 17, 21
IT11	0.14	21	1, 5, 7, 10, 14, 18, 21

Table VI. Normalized mass loss ($\times 10^{-2}$ $g \cdot m^{-2}$) at 90°C for glass sample IT1

Time (d)	NL(Si)	NL(B)	NL(Na)	NL(Li)	NL(Mo)	NL(Al)	NL(Ca)	NL(Sr)	NL(Zn)	NL(Fe)
0.10	3	101	135	80	161	nd	72	578	nd	nd
5.00	86	258	186	96	185	nd	209	135	nd	nd
6.91	147	221	139	201	192	nd	146	142	nd	nd
9.89	222	284	250	268	239	nd	235	212	nd	nd
13.96	311	464	363	390	268	nd	353	308	nd	nd
20.89	372	473	384	479	341	nd	359	362	nd	nd
27.89	444	517	458	76	409	396	524	412	10	74

Table VII. Normalized mass loss ($\times 10^{-2}$ $g \cdot m^{-2}$) at 90°C for glass sample IT2

Time (d)	NL(Si)	NL(B)	NL(Na)	NL(Li)	NL(Mo)	NL(Al)	NL(Ca)	NL(Sr)	NL(Zn)	NL(Fe)
0.30	148	223	219	217	251	177	251	202	5	262
0.96	470	525	501	526	534	333	523	294	3	63
1.34	644	743	721	749	731	346	621	813	6	66
1.89	920	1067	1033	1074	1060	371	890	292	3	63
2.28	1022	1201	1161	1207	1219	537	975	1180	4	204
2.90	1287	1549	1480	1627	1553	516	1177	1349	3	62
3.18	1333	1623	1583	1617	1662	543	1388	1436	3	62
5.91	2054	2875	2753	2982	2890	180	1668	1845	4	214

Table VIII. Normalized mass loss (× 10^{-2} g·m^{-2}) at 90°C for glass sample IT3

Time (d)	NL(Si)	NL(B)	NL(Na)	NL(Li)	NL(Mo)	NL(Al)	NL(Ca)	NL(Sr)	NL(Zn)	NL(Fe)
0.29	31	25	90	77	127	53	79	103	1.22	94
0.96	109	76	181	177	122	72	140	169	0.80	64
1.35	159	133	221	221	153	75	163	208	1.58	67
1.90	230	181	276	279	219	112	215	297	0.89	64
2.28	273	253	334	326	298	219	339	303	1.24	92
2.89	359	311	388	400	337	242	362	440	0.82	89
3.16	420	378	456	459	438	378	640	524	17.7	109
5.92	702	677	744	734	699	617	636	785	0.96	229

Table IX. Normalized mass loss (× 10^{-2} g·m^{-2}) at 90°C for glass sample IT4

Time (d)	NL(Si)	NL(B)	NL(Na)	NL(Li)	NL(Mo)	NL(Al)	NL(Ca)	NL(Sr)	NL(Zn)	NL(Fe)
0.08	20	44	33	27	190	10	21	<101	0.23	157
0.31	28	35	50	29	49	31	65	0	9	110
0.90	140	153	152	121	187	123	220	0.5	23	85
1.33	237	259	241	223	269	215	224	118	28	32
1.90	338	377	342	316	374	282	303	198	25	43
2.34	451	505	460	439	504	373	380	306	24	38
2.91	548	620	572	539	612	442	476	389	21	35
3.19	621	706	658	619	720	483	522	399	20	47

Table X. Normalized mass loss (× 10^{-2} g·m^{-2}) at 90°C for glass sample IT5

Time (d)	NL(Si)	NL(B)	NL(Na)	NL(Li)	NL(Mo)	NL(Al)	NL(Ca)	NL(Sr)	NL(Zn)	NL(Fe)
0.07	53	45	53	17	340	20	63	99	6	107
0.31	192	203	203	149	264	155	191	215	16	63
0.89	1019	1313	1228	1142	1309	703	690	746	28	66
1.09	1208	1621	1548	1445	1605	695	544	726	35	47
1.32	1575	2274	2115	2021	2262	751	534	708	31	46
1.90	2460	4496	4126	3959	4453	784	215	300	30	42
2.09	2721	5318	4890	4746	5275	775	188	401	26	49
2.34	3083	6388	5855	5720	6393	786	157	391	26	174

Table XI. Normalized mass loss (× 10^{-2} g·m^{-2}) at 90°C for glass sample IT6

Time (d)	NL(Si)	NL(B)	NL(Na)	NL(Li)	NL(Mo)	NL(Al)	NL(Ca)	NL(Sr)	NL(Zn)	NL(Fe)
0.10	0	4	21	13	20	nd	7	82	nd	nd
0.88	16	4	84	13	20	nd	23	82	nd	nd
2.88	57	31	41	59	19	nd	185	77	nd	nd
6.89	111	131	56	87	119	nd	66	81	nd	nd
9.04	138	149	131	147	138	nd	114	80	nd	nd
13.99	194	201	178	197	186	nd	147	75	nd	nd
17.00	218	224	208	232	223	nd	173	76	nd	nd
20.95	247	261	248	266	367	219	217	79	12	173

Table XII. Normalized mass loss (× 10^{-2} g·m^{-2}) at 90°C for glass sample IT7

Time (d)	NL(Si)	NL(B)	NL(Na)	NL(Li)	NL(Mo)	NL(Al)	NL(Ca)	NL(Sr)	NL(Zn)	NL(Fe)
0.07	52	9	27	32	130	5	17	105	14	176
0.32	160	9	30	31	124	49	46	100	13	389
0.88	156	39	110	78	177	88	164	612	14	162
1.36	224	49	146	122	246	137	170	694	13	250
1.90	235	73	198	186	350	177	501	1109	13	163
2.35	254	84	235	214	419	195	201	1392	13	132
2.92	281	101	299	233	477	125	268	1520	14	82
3.36	347	104	306	269	554	291	271	1945	13	208
3.90	326	118	330	300	600	297	268	1675	12	54

Table XIII. Normalized mass loss (× 10^{-2} g·m^{-2}) at 90°C for glass sample IT8

Time (d)	NL(Si)	NL(B)	NL(Na)	NL(Li)	NL(Mo)	NL(Al)	NL(Ca)	NL(Sr)	NL(Zn)	NL(Fe)
0.30	135	258	145	249	69	106	193	206	78	67
0.96	513	718	564	800	480	471	530	695	75	64
1.35	615	803	661	947	582	488	589	720	78	67
1.90	726	905	774	1072	716	535	748	882	74	114
2.30	745	925	796	1091	758	679	724	898	75	246
2.90	801	998	849	1179	834	663	781	975	73	63
3.17	822	1025	947	1212	863	720	1242	957	72	112
5.92	921	1136	1007	1337	971	828	1034	968	73	238

Table XIV. Normalized mass loss ($\times 10^{-2}$ g·m^{-2}) at 90°C for glass sample IT9

Time (d)	NL(Si)	NL(B)	NL(Na)	NL(Li)	NL(Mo)	NL(Al)	NL(Ca)	NL(Sr)	NL(Zn)	NL(Fe)
0.09	196	212	183	165	163	nd	152	105	nd	nd
0.21	519	587	539	519	447	nd	459	219	nd	nd
0.88	908	1118	1038	1001	967	nd	723	631	nd	nd
1.11	919	1161	1068	1023	991	nd	738	537	nd	nd
1.88	946	1160	1102	1108	1005	nd	754	312	nd	nd
2.03	949	1197	1101	1093	990	nd	782	410	nd	nd
2.20	1414	1191	1101	1070	992	nd	766	402	nd	nd
2.88	951	1219	1127	1096	1020	nd	745	411	nd	nd
3.16	954	1207	1127	1110	1024	nd	754	494	nd	nd

Table XV. Normalized mass loss ($\times 10^{-2}$ g·m^{-2}) at 90°C for glass sample IT10

Time (d)	NL(Si)	NL(B)	NL(Na)	NL(Li)	NL(Mo)	NL(Al)	NL(Ca)	NL(Sr)	NL(Fe)	NL(Zn)
0.27	216	45	682	647	115	1371	378	nd	nd	nd
0.93	453	226	1650	1682	277	2880	543	nd	nd	nd
1.31	509	481	1863	1943	319	3202	543	nd	nd	nd
1.96	532	555	2027	2009	341	3357	518	nd	nd	nd
2.23	569	579	2165	2129	360	3666	600	nd	nd	nd
2.95	551	649	2124	2173	357	3402	481	nd	nd	nd
3.28	579	588	2211	2321	370	3596	498	nd	nd	nd
3.68	670	674	2238	2255	370	3528	454	nd	nd	nd

Table XVI. Normalized mass loss ($\times 10^{-2}$ g·m^{-2}) at 90°C for glass sample IT11

Time (d)	NL(Si)	NL(B)	NL(Na)	NL(Li)	NL(Mo)	NL(Al)	NL(Ca)	NL(Sr)	NL(Zn)	NL(Fe)
0.10	2	9	26	1	7	0	30	29	0	0
5.00	122	228	232	117	101	-	182	73	-	-
6.96	194	248	235	177	141	-	238	168	-	-
9.89	275	337	310	271	201	-	328	229	-	-
13.96	331	436	540	349	255	-	378	289	-	-
17.89	381	441	420	391	273	-	353	326	-	-
20.89	413	506	457	442	304	297	402	337	32	182

Table XVII. Normalized mass loss (× 10^{-2} g·m^{-2}) at 90°C for glass sample IT12

Time (d)	NL(Si)	NL(B)	NL(Na)	NL(Li)	NL(Al)	NL(Ca)	NL(Sr)	NL(Zn)	NL(Fe)
0.07	8	20	19	0	48	17	6	870	nd
0.30	40	47	52	20	57	18	31	54	nd
0.90	263	346	322	208	233	262	19	72	nd
1.09	310	409	386	255	255	291	19	29	nd
1.32	349	484	455	305	285	325	15	29	nd
1.91	425	616	585	393	351	398	15	42	nd
2.10	445	657	623	416	356	412	15	39	nd
2.33	466	698	660	448	373	424	15	35	182

Table XVIII. Normalized mass loss (× 10^{-2} g·m^{-2}) at 90°C for glass sample IT13

Time (d)	NL(Si)	NL(B)	NL(Na)	NL(Li)	NL(Mo)	NL(Al)	NL(Ca)	NL(Sr)	NL(Zn)	NL(Fe)
0.19	1156	1854	1829	1646	1730	nd	571	485	nd	nd
0.83	4242	8907	8547	7803	8029	nd	520	579	nd	nd
1.07	5402	12202	11689	10707	11078	nd	504	474	nd	nd
1.18	5593	12844	12205	11106	11900	nd	334	363	nd	nd
1.80	7120	17777	16826	15385	16072	nd	255	265	nd	nd
1.98	7543	19423	18301	16800	17742	nd	259	216	nd	nd
2.09	7770	20179	18967	17451	18717	1706	188	207	149	511

Table XIX. Normalized mass loss (× 10^{-2} g·m^{-2}) at 90°C for glass sample IT14

Time (d)	NL(Si)	NL(B)	NL(Na)	NL(Li)	NL(Mo)	NL(Al)	NL(Ca)	NL(Sr)	NL(Zn)	NL(Fe)
0.28	57	77	70	96	72	nd	33	42	nd	nd
0.91	308	397	671	436	374	nd	228	303	nd	nd
1.25	417	566	560	600	506	nd	331	430	nd	nd
1.89	546	791	753	812	700	nd	443	567	nd	nd
2.18	582	863	813	877	766	nd	494	599	nd	nd
2.89	664	1050	988	1051	976	nd	544	672	nd	nd
3.22	686	1122	1083	1117	1008	454	644	714	8	66

Table XX. Normalized mass loss ($\times 10^{-2}$ g·m^{-2}) at 90°C for glass sample IT15

Time (d)	NL(Si)	NL(B)	NL(Na)	NL(Li)	NL(Mo)	NL(Al)	NL(Ca)	NL(Sr)	NL(Zn)	NL(Fe)
0.09	50	66	57	0	63	5	4	18	76	1826
0.33	387	102	75	1	64	14	505	28	77	290
0.92	235	113	81	32	64	66	352	75	77	344
1.36	381	143	98	75	74	101	105	126	74	178
1.91	331	201	162	123	151	144	207	183	75	285
2.37	463	224	186	153	150	184	220	254	75	244
2.91	288	252	248	186	177	217	273	257	76	299
3.37	463	265	236	206	194	238	238	246	72	162
3.93	337	301	267	244	236	280	357	291	71	158

Table XXI. Normalized mass loss ($\times 10^{-2}$ g·m^{-2}) at 90°C for glass sample IT16

Time (d)	NL(Si)	NL(B)	NL(Na)	NL(Li)	NL(Mo)	NL(Al)	NL(Ca)	NL(Sr)	NL(Zn)	NL(Fe)
0.09	8	15	28	0	6	0	80	24	69	0
0.34	31	30	30	0	25	19	84	25	49	26
0.93	124	131	434	22	121	92	216	109	62	74
1.38	191	195	669	109	177	149	186	174	56	23
1.94	256	265	939	161	244	197	257	254	50	43
2.39	296	315	1254	230	277	228	288	293	41	32
2.93	341	366	1552	283	332	279	325	349	34	36
3.23	371	399	1783	323	362	298	348	392	26	16

Table XXII. Normalized mass loss ($\times 10^{-2}$ g·m^{-2}) at 90°C for glass sample IT17

Time (d)	NL(Si)	NL(B)	NL(Na)	NL(Li)	NL(Mo)	NL(Al)	NL(Ca)	NL(Sr)	NL(Zn)	NL(Fe)
0.26	99	119	160	112	113	81	123	125	78	67
0.90	318	384	430	379	369	288	362	341	72	62
1.13	370	459	496	446	452	294	443	425	73	63
1.88	442	567	577	555	529	339	522	469	74	63
2.25	463	601	634	587	594	415	538	522	76	65
2.88	500	648	707	641	621	400	556	582	73	63
3.14	514	664	725	670	667	442	888	619	73	75
5.90	558	762	814	758	744	503	616	644	76	287

Table XXIII. Normalized mass loss (× 10^{-2} g·m^{-2}) at 90°C for glass sample IT18

Time (d)	NL(Si)	NL(B)	NL(Na)	NL(Li)	NL(Mo)	NL(Al)	NL(Ca)	NL(Sr)	NL(Zn)	NL(Fe)
0.08	7	7	32	45	8	0	20	33	18	0
0.33	33	30	36	48	35	20	67	35	116	159
0.93	128	136	140	66	525	96	178	108	132	1958
1.37	180	187	182	139	192	147	173	170	87	102
1.94	234	249	252	189	247	192	235	242	76	143
2.38	284	309	305	262	308	235	281	304	62	102
2.93	344	378	372	337	373	294	351	370	49	89
3.23	384	432	426	400	425	326	367	423	48	49

Table XXIV. Normalized mass loss (× 10^{-2} g·m^{-2}) at 90°C for glass sample IT19

Time (d)	NL(Si)	NL(B)	NL(Na)	NL(Li)	NL(Mo)	NL(Al)	NL(Ca)	NL(Sr)	NL(Zn)	NL(Fe)
0.10	22	14	41	0	45	11	0	0	415	1324
0.33	386	35	27	0	46	26	346	1	299	119
0.90	313	167	162	104	84	160	261	153	440	156
1.38	559	281	235	206	188	255	238	219	483	100
1.92	428	402	335	303	294	327	388	411	498	142
2.37	615	484	402	373	436	410	384	444	558	146
2.92	462	537	468	442	496	450	419	587	-95	111
3.38	705	579	501	474	545	480	445	465	600	109
3.91	551	623	537	536	562	514	474	492	465	102

Table XXV. Normalized mass loss (× 10^{-2} g·m^{-2}) at 90°C for glass sample IT20

Time (d)	NL(Si)	NL(B)	NL(Na)	NL(Li)	NL(Mo)	NL(Al)	NL(Ca)	NL(Sr)	NL(Zn)	NL(Fe)
0.09	23	28	46	4	15	14	40	23	21	37
0.33	181	207	192	137	182	157	190	125	124	187
0.91	484	596	546	486	501	454	355	406	63	216
1.11	555	691	642	585	597	527	396	441	61	156
1.36	607	747	699	639	626	567	416	462	60	142
1.93	691	889	851	791	745	676	461	542	73	75
2.12	681	892	842	772	733	648	463	507	60	141
2.38	712	942	895	809	788	673	469	526	104	140

Table XXVI. Normalized mass loss (× 10^{-2} g·m^{-2}) at 90°C for glass sample $R7T7_{max}$

Time (d)	NL(Si)	NL(B)	NL(Na)	NL(Li)	NL(Mo)	NL(Al)	NL(Ca)	NL(Sr)	NL(Zn)	NL(Fe)
0.28	49	65	53	40	55	29	58	45	44	37
0.88	192	206	207	190	180	150	188	258	28	187
1.15	258	291	274	258	256	201	373	326	24	216
1.89	453	500	511	479	470	359	405	523	24	156
2.27	530	613	584	583	574	398	442	662	24	142
2.89	667	763	751	740	730	510	555	862	23	75
3.16	738	862	1057	831	821	552	982	901	47	141
5.91	885	1086	1062	1056	1070	562	717	1047	24	140

Table XXVII. Normalized mass loss (× 10^{-2} g·m^{-2}) at 90°C for glass sample $R7T7_{min}$

Time (d)	NL(Si)	NL(B)	NL(Na)	NL(Li)	NL(Mo)	NL(Al)	NL(Ca)	NL(Sr)	NL(Zn)	NL(Fe)
0.28	2	18	59	30	56	16	28	35	59	37
0.93	58	76	131	73	76	53	101	51	33	187
1.16	75	80	117	86	86	61	215	77	14	216
1.88	120	112	134	116	108	92	100	121	14	156
2.28	144	133	171	146	142	118	136	122	15	142
2.90	193	176	229	185	181	167	200	141	14	75
3.16	201	183	211	199	191	166	187	162	14	141
5.90	320	313	357	332	324	264	272	296	14	140

Table XXVIII. Normalized mass loss (× 10^{-2} g·m^{-2}) at 90°C for glass sample R7T7

Time (d)	NL(Si)	NL(B)	NL(Na)	NL(Zn)	NL(Al)	NL(Ca)	NL(Mo)	NL(Sr)	NL(Fe)	NL(Li)
0.42	14	30	15	19	16	57	nd	nd	nd	nd
0.53	15	17	18	16	16	83	nd	nd	nd	nd
0.76	26	23	25	19	19	50	nd	nd	nd	nd
0.99	23	24	28	20	22	149	nd	nd	nd	nd
1.22	28	49	37	27	21	300	nd	nd	nd	nd
1.45	33	39	40	24	19	73	nd	nd	nd	nd
1.68	37	40	40	27	24	183	nd	nd	nd	nd
1.91	42	47	54	30	25	124	nd	nd	nd	nd
2.14	43	48	57	29	34	152	nd	nd	nd	nd
2.36	47	70	44	31	34	65	nd	nd	nd	nd
2.59	50	58	42	34	33	92	nd	nd	nd	nd
2.82	55	56	50	35	37	129	nd	nd	nd	nd
3.05	58	57	53	40	41	78	nd	nd	nd	nd
5.90	113	109	82	44	79	107	nd	nd	nd	nd

Table XXIX. Initial dissolution mechanisms (refer to text: § 4.4.1, page 13)

Glass sample	Duration (days)	B	Na	Li	Mo	Al	Ca	Initial-final pH
IT1	27.89	I(+)	I(+)	I(+)	I(+;5) C	*	I(+;5) C	6.04 -8.41
IT2	5.90	I(+)	I(+)	I(+)	I(+;0.3) C°	I(+;0.3) C	I(+;0.96) C	5.88-8.97
IT3	6.38	C	I(+)	I(+)	I(+;0.28) C	I(+;0.28) C	I(+;0.28)/ C	5.78-9.32
IT4	2.91	I(+;0.31) C	I(+)	I(+;0.31) C	I(+;0.31) C	I(+;0.9) C	I(+;1.33) C	6.60-8.95
IT5	2.34	C(0.31) I(+)	C(0.31) I(+)	I(+ ; 0.31) C	I(+)	I(-)	I(+;0.31) I(-)	7.01-9.63
IT6	20.95	I(+;0.88) I(-;2.88)C	I(+;0.88) I(-;1.36)C	I(+;0.1) C	C	*	I(+;2.881) C	6.63-3.91
IT7	3.90	I(-)	I(-;2.92) C	I(-)/C	I(+;0.07) C	I(-;3.36) C	I(-)/C	6.60-8.95
IT8	5.92	I(+)	I(+)	I(+)	I(+)	I(+)	I(+)	5.78-9.38
IT9	3.16	I(+)	I(+)	I(+)	C	*	I(-)	
IT10a	3.68	I(-)/C	I(+)	I(+)	I(-)	I(+)	I(+)	7.50-9.01
IT11	20.89	I(+)	I(+)	C	I(+;0.1) I(-)	*	I(+)	6.04-8.50
IT12	2.33	I(+)	I(+)	I(+;0.07) C	*	C	I(+.0.3)C I(-)	6.47-9.12
IT13	2.09	I(+)	I(+)	I(+)	I(+)	*	I(-)	6.79-9.8
IT14	3.22	I(+)	I(+)	I(+)	I(+)	*	I(-)/C	6.04-8.05
IT15	3.93	I(+;0.09) I(-)	I(+;0.09) I(-)	I(-)	I(+;0.09) I(-)	I(-)	I(-)	6;14-7.95
IT16	3.23	I(+)	I(+)	I(-)	C	I(-)	I(+)	6.1-7.53
IT17	5.90	I(+)	I(+)	I(-)	I(+)	C	I(+)	5.85-8.57
IT18	3.23	I(-;0.33)C I(+)	I(+)	C	C	I(-)	I(+;1.37) C	7.03-7.85
IT19	3.38	I(-;1.92) C	I(+;0.1) I(-)C	I(-)	I(+;0.1) I(-)C	I(-)	I(-)	7.2-9.79
IT20	2.38	I(+)	I(+)	C	C	I(-)/C	I(-)	6.63-9.17
$R7T7_{max}$	5.91	I(+)	I(+)	I(+;0.28) C	I(+;0.28) C	I(+;0.28) C	I(+;1.16) C	5.88-9.13
$R7T7_{min}$	5.90	I(+)	I(+)	*	I(+)	I(+;0.28) I(-)	I(+)	5.90-8.50
R7T7	5.90	I(+)	I(+)	*	*	I(+) C	*	5.13-7.58

Table XXX. Initial dissolution rates (r_0) calculated from normalized mass losses

Glass	Duration (days)	Mean pH	r_0(Si) ($g \cdot m^{-2} d^{-1}$)	r_0(B ($g \cdot m^{-2} d^{-1}$)	r_0(Na ($g \cdot m^{-2} d^{-1}$)	r_0(Li ($g \cdot m^{-2} d^{-1}$)	r_0(Mo ($g \cdot m^{-2} d^{-1}$)
IT1	14.00	7.79	0.23 ±0.01	0.24 ±0.05	0.16 ±0.05	0.23 ±0.04	0.08 ±0.01
IT2	2.28	7.99	3.4 ±0.2	4.7 ±0.07	4.5 ±0.08	4.9 ±0.10	4.7 ±0.07
IT3	5.92	8.33	1.2 ±0.03	1.2 ±0.03	1.2 ±0.03	1.2 ±0.03	1.1 ±0.06
IT4	3.19	8.39	2.0 ±0.04	2.2 ±0.07	2.0 ±0.05	2.0 ±0.06	1.9 ±0.18
IT5	1.32	8.93	12.4 ±0.7	17.8 ±1.4	16.6 ±1.3	16.0 ±1.3	15.7 ±2.1
IT6	20.95	3.97	0.12 ±0.006	0.13 ±0.008	0.10 ±0.01	0.13 ±0.005	0.15 ±0.012
IT7	3.9	7.6	0.9 ±0.3	0.4 ±0.03	1.0 ±0.07	0.9 ±0.09	1.2 ±0.18
IT8	1.9	8.62	2.4 ±0.5	4.0 ±1.0	3.9 ±1.5	5.1 ±2.1	4.0 ±1.4
IT9	0.88	8.53	8.0 ±5.1	10.3 ±5.6	9.8 ±5.4	9.5 ±5.4	9.4 ±3.9
IT10a	1.3	8.76	2.9 ±1.0	4.0 ±1.9	11.8 ±4.3	12.9 ±4.2	2.0 ±0.62
IT11	13.96	7.94	0.25 ±0.02	0.30 ±0.03	0.35 ±0.04	0.26 ±0.01	0.18 ±0.008
IT12	1.32	8.49	2.1 ±0.2	3.1 ±0.2	2.9 ±0.2	2.0 ±0.11	
IT13	2.09	9.22	32.9 ±3.1	94.1 ±4.6	87.9 ±4.1	81.0 ±4.2	86.5 ±4.2
IT14	1.89	7.94	2.0 ±0.3	3.5 ±0.3	2.9 ±0.5	3.3 ±0.3	3.1 ±0.2
IT15	3.93	7.52	1.0 ±0.9	0.7 ±0.1	0.5 ±0.1	0.7 ±0.08	0.4 ±0.2
IT16	3.23	7.62	1.2 ±0.04	1.2 ±0.04	5.7 ±0.2	1.1 ±0.06	1.1 ±0.04
IT17	1.13	7.86	3.2 ±0.4	4.0 ±0.3	4.0 ±0.5	3.9 ±0.5	4.0 ±0.1
IT18	3.23	7.68	1.2 ±0.02	1.3 ±0.02	1.2 ±0.02	1.1 ±0.08	1.0 ±0.4
IT19	1.92	8.41	1.9 ±1.1	2.2 ±0.09	1.7 ±0.2	1.8 ±0.1	1.4 ±0.2
IT20	1.11	8.60	5.2 ±0.4	6.5 ±0.4	5.9 ±0.2	5.8 ±0.2	5.6 ±0.3
$R7T7_{max}$	2.89	8.19	2.4 ±0.05	2.7 ±0.05	2.7 ±0.07	2.7 ±0.05	2.7 ±0.07
$R7T7_{min}$	5.9	7.62	0.56 ±0.02	0.51 ±0.02	0.51 ±0.03	0.54 ±0.008	0.49 ±0.02
R7T7		6.24	0.18 ±0.006	0.16 ±0.006	0.12 ±0.01	nd	nd

Table XXXI. Variance analysis for r_0(B)

Source of variation	Sum of squares of variation sources	Degrees of freedom	Mean squares	Ratio of mean squares to error mean square	Significance
Regression	117.93	10	11.79	7.63	100%
Residue	35.53	23	1.54		
Validity	16.27	7	2.32	1.5	21.5%
Error	35.53	23	1.54		
Total	153.46	40			

Table XXXII. Major oxide concentrations (wt%) in glass compositions used to test the model

Glass	SiO_2	Al_2O_3	B_2O_3	Na_2O + Li_2O	CaO	Additive oxides	FP + act oxides + ZrO_2
$R7T7_{max}$	42.40	3.60	16.50	13.40	4.8	8.29	11.01
$R7T7_{min}$	51.70	6.60	12.40	9.70	3.5	3.79	12.31
R7T7	45.48	4.91	14.02	11.84	4.04	6.94	12.77
$R7T7_{-10\%}$	35.12	5.76	16.46	13.89	4.74	7.75	16.28
$R7T7_{+5\%}$	50.12	4.43	12.65	10.68	3.64	5.95	12.53
$R7T7_{+10\%}$	55.12	3.98	11.38	9.61	3.28	5.37	11.26
$R7T7_{+15\%}$	60.12	3.54	10.12	8.54	2.91	4.76	10.01
$R7T7_{4\%Mo}$	42.90	4.34	16.5	10.63	3.47	6.69	15.47
M7	42.98	3.71	16.62	13.44	3.54	6.62	13.09

Table XXXIII. Experimental (exp) versus calculated (calc) initial dissolution rates for all 29 glass compositions tested

Glass	r_0(B) exp ($g \cdot m^{-2} d^{-1}$)	r_0(B) calc ($g \cdot m^{-2} d^{-1}$)	Residue ($g \cdot m^{-2} d^{-1}$)	Residue (%)
IT1	0.24	0.45	–0.21	87.5
IT2	4.74	4.57	0.17	3.6
IT3	1.19	1.23	–0.04	3.3
IT4	2.21	1.91	0.3	13.5
IT5	17.78	6.84	10.94	61.5
IT6	0.13	–0.16	0.29	n.s
IT7	0.36	1.44	–1.08	n.s
IT8	4.00	4.22	–0.22	5.5
IT9	10.35	8.52	1.83	17.7
IT10	4.04	4.29	–0.25	6.2
IT11	0.30	0.16	0.14	52.6
IT12	3.12	4.76	–1.64	90.1
IT13	94.14	9.31	84.83	28
IT14	3.47	2.50	0.97	10.4
IT15	0.67	0.73	–0.07	n.s
IT16	1.25	–0.76	2.01	4.5
IT17	3.97	3.79	0.18	n.s
IT18	1.32	3.12	–1.80	29.5
IT19	2.20	2.85	–0.65	1.22
IT20	6.53	6.45	0.08	15.0
$R7T7_{max}$	2.74	3.15	–0.41	n.s
$R7T7_{min}$	0.51	1.68	–1.17	n.s
R7T7	0.16	2.25	–2.09	n.s
$R7T7_{-10\%}$	1.30	3.51	–2.21	n.s
$R7T7_{+5\%}$	0.56	1.76	–1.20	n.s
$R7T7_{+10\%}$	0.55	1.35	–0.80	n.s
$R7T7_{+15\%}$	0.58	1.04	–0.46	n.s
$R7T7_{4\%Mo}$	0.88	2.67	–1.79	n.s
M7	0.699	3.32	–2.62	n.s

Table XXXIV. Glass dissolution at 90°C and 200 cm^{-1}: Principal test results

1	2	3	4	5	6	7	8
Glass	NL(B) after 182 days ($g \cdot m^{-2}$)	Final rate ($\times 10^{-2}$ $g \cdot m^{-2} d^{-1}$)	Initial rate ($g \cdot m^{-2} d^{-1}$)	Si ($mg \cdot l^{-1}$)	H4SiO4° ($mol \cdot l^{-1}$)	Molecular weight ($g \cdot mol^{-1}$)	pH after 182 days
IT15	0.09	0.01	0.70	45		80.40	9.83
IT 1	0.13	0.03	0.24	305		63.10	9.6
$R7T7_{min}$	0.28	9.9	0.51	110	$10^{-2.84}$	68.30	9.20
IT19	0.44	0.14	2.20	140		70.40	10.1
R7T7	0.59	0.8	0.16	132	$10^{-3.01}$	69.40	9.50
IT18	0.65	0.26	1.30	20	$10^{-3.39}$	75.10	8.65
IT7	0.76	0.32	0.40	26.7		72.50	8.5
IT2	1.20	0.13	4.70	210	$10^{-2.40}$	64.20	8.8
IT14	1.28	0.29	3.50	52		77.80	8.88
IT17	1.36	0.39	4.0	30		77.60	8.81
IT16	1.95	0.85	1.20	37		80.30	9.90
$R7T7_{max}$	4.68	2.2	2.70	310	$10^{-2.76}$	68.70	9.50
IT12	6.01	2.71	3.10	993		74.60	11.3
IT6	7.72	0.008	0.13	114		68.30	9.4
IT13	9.58	0.76	94.1	1000–2000		68.70	11.1
IT9	15.8	9.47	10.3	167		66.20	10.8
IT8	16.3	8.72	4.0	270		66.60	11.2
IT5	17.1	1.98	17.8	2587		64.60	10.6
IT10	17.7	0.06	4.0	64	$10^{-3.42}$	69.10	9.5
IT3	19.6	1.06	1.20	5050		61.60	11.0
IT20	20.4	7.69	6.50	431		71.80	11.4
IT11	20.7	0.03	0.30	240	$10^{-3.07}$	73.00	9.8
IT4	20.8	2.73	2.2.	6530		63.40	11.3

LIST OF FIGURES

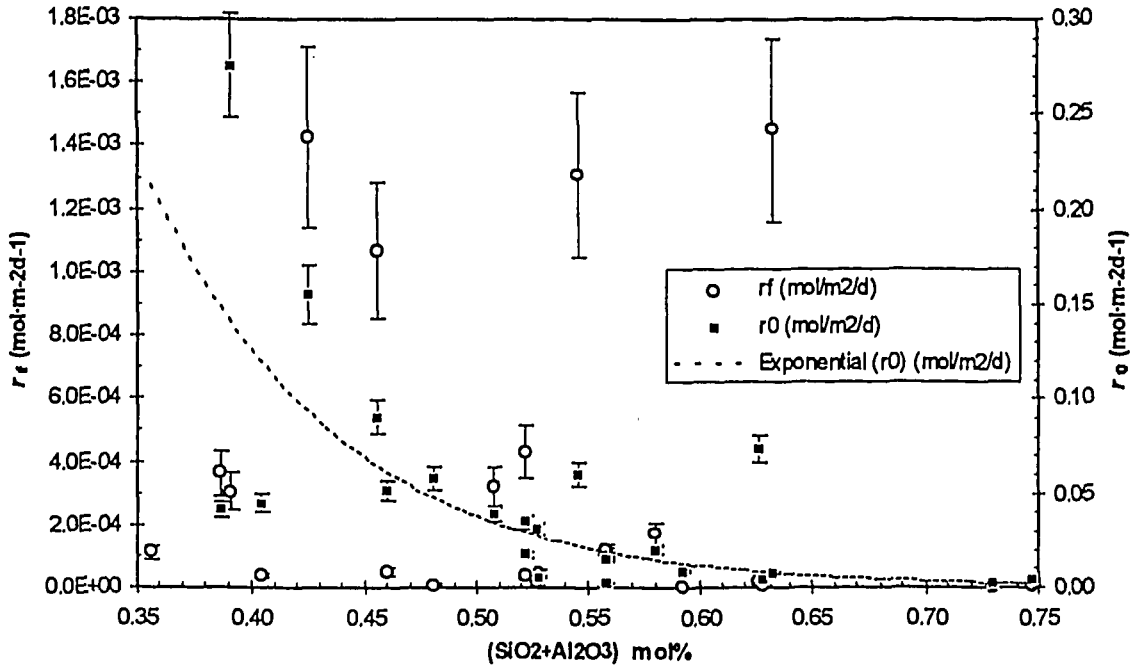

Figure 1. Molar percentage of $(SiO_2 + Al_2O_3)$ in the glass versus the initial corrosion rate (r_0) and the long-term corrosion rate (r_f) at 90°C; corrosion rates are expressed in mol·m^{-2}d^{-1}

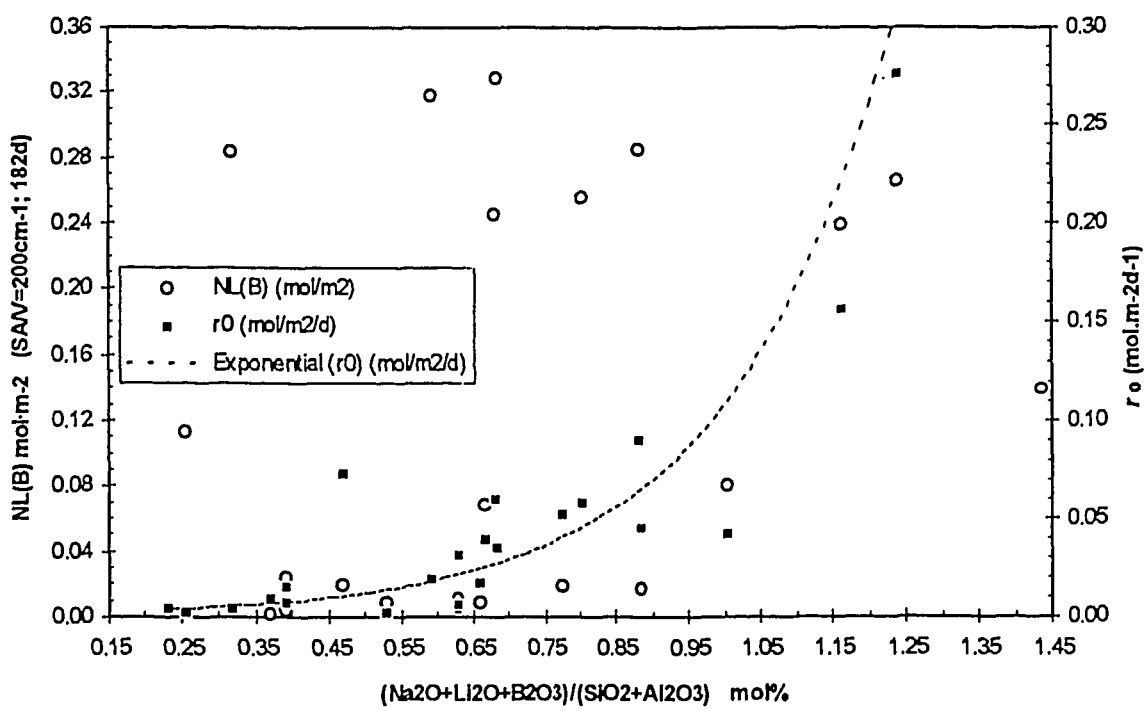

Figure 2. $(Na_2O + Li_2O + B_2O_3)$ / $(SiO_2 + Al_2O_3)$ molar ratio in the glass versus the initial corrosion rate at 90°C (r_0) and the normalized boron mass loss (NL(B)) at 90°C after 182 days at 200 cm^{-1}; corrosion rates are expressed in mol·m^{-2}d^{-1} and normalized mass losses in mol·m^{-2}

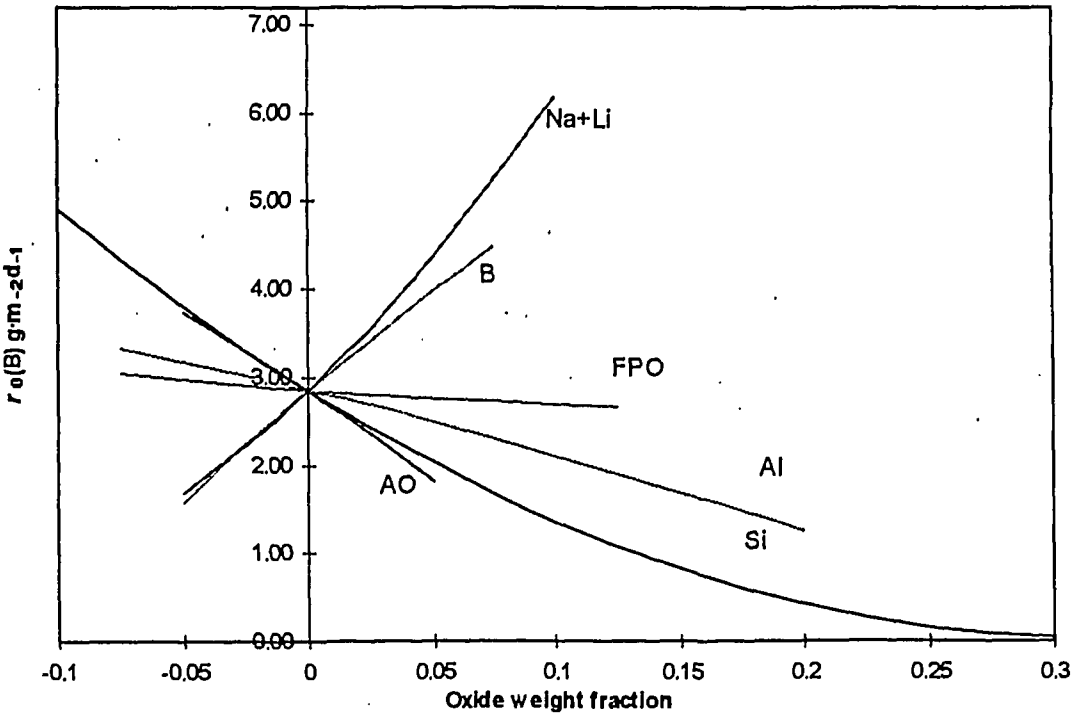

Figure 3. Effects of various oxides on the initial corrosion rate r_0 ($g \cdot m^{-2} d^{-1}$) at 90°C

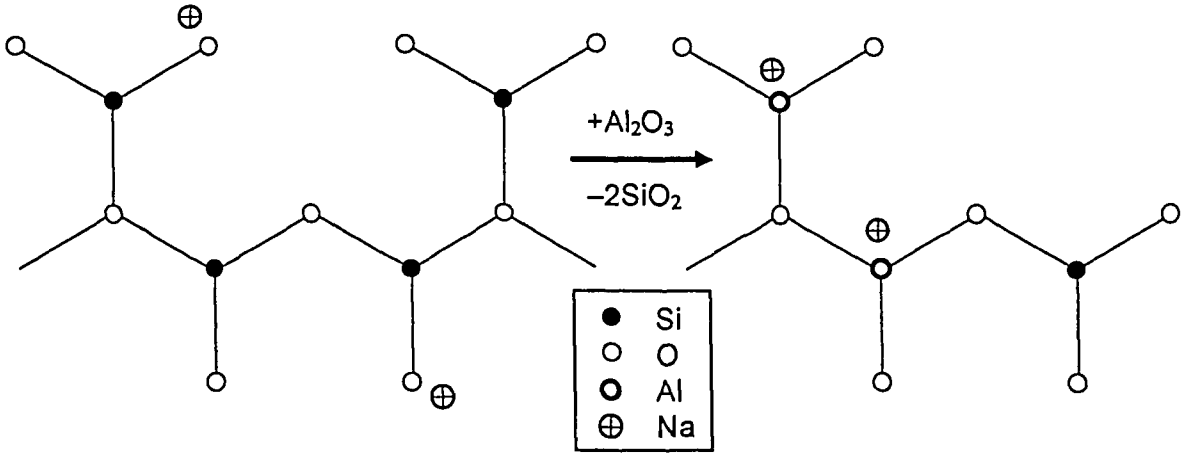

Figure 4. Schematic representation of the replacement of SiO_2 by Al_2O_3 in a sodium silicate glass[18]